Drew University

College of Liberal Arts

The Heterogeneous Reaction of Isoprene and Kaolinite

By
Theresa M. Kucinski

Submitted in the Fulfillment
Of the Requirements
For the Degree of
Bachelor in Arts
With Specialized Honors in Chemistry
May 2016

Committee Members*:*
Dr. Ryan Z. Hinrichs
Dr. Adam Cassano
Dr. Lisa Jordan
Dr. Michael Peglau

Acknowledgements

I would like to take a moment to acknowledge all of the people who supported this project. I would like to first thank Dr. Ryan Hinrichs for his continued guidance throughout my two years at Drew University as well as for introducing me to the wonderful world of atmospheric chemistry. I had a great time constructing and figuring out the laminar flow reactor together while learning a lot in the process. I would also like to thank my committee members; Dr. Adam Cassano, Dr. Lisa Jordan, and Dr. Michael Peglau who have been a great support system throughout my writing process. A special thank you goes out to my family for always contributing their presence and support, even during the uphill climbs. Finally, I would like to thank my friends at Drew, the entirety of the Chemistry Department, and Howard Fraenkel, for their aid and encouragement that helped me throughout my research.

Abstract

Isoprene is the most abundant biogenic volatile organic compound (BVOC) in the Earth's atmosphere with emissions levels second only to methane. Once in the atmosphere, isoprene can undergo oxidation reactions and yield products that condense to form secondary organic aerosols (SOA), however there is still uncertainty over these processes. For example, there is still a discrepancy between model estimations and field measurements of isoprene concentration, especially over forest canopies. We suggest the reactive uptake of isoprene on mineral solids in soil as a possible sink. A laminar flow reactor was constructed to study the heterogeneous reaction of isoprene and kaolinite. The isoprene and kaolinite reaction produced adsorbed organic compounds that are suggested to be 2-c-methyl-eryhtritol and possibly the 2-methylthreitol, isomers of the 2-methyl tetrol and a component detected in aerosols. Kinetic analysis with the use of a laminar flow reactor provided an initial effective reactive uptake coefficient 1.3×10^{-4} for the heterogeneous reaction of isoprene and kaolinite under dry conditions. Further analysis under relative humidity is required to determine atmospheric relevance. If uptake coefficients remain on the same order of magnitude under humidified conditions, then this reaction would be considered a significant atmospheric process.
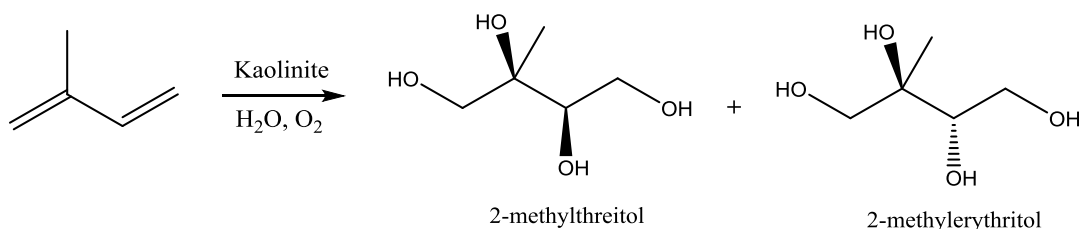
Scheme A. The suggested heterogeneous reaction of isoprene and kaolinite produces the 2-methyl tetrol isomers.

Abstract

Table of Contents

Terminology

Terminology

2-C-methyl-eryhtritol: An isomer of the 2-methyl tetrol

BVOC: biogenic volatile organic compounds that are emitted from vegetation.

Cloud Condensation Nucleus: A particle that provides a surface for water to condense upon.

DRIFTS: Diffuse reflectance infrared spectroscopy. A method used here to monitor the growth of organic compounds on mineral surfaces.

GC-MS: Gas chromatography mass spectroscopy

Heterogeneous Reaction: The reaction between a gaseous and solid compound.

Ice Nucleus: A particle that provides a surface for formation of ice in the atmosphere.

Isomer: A molecule with the same molecular formula but with a different arrangement of atoms.

Kaolinite: A clay mineral.

Methane: A greenhouse gas

PPB: parts per billion

PPM: parts per million

Radiative Forcing: The difference of light being absorbed and radiated back to space.

Residence Time: Amount of time a particle is in a given system.

SOA: secondary organic aerosol, produced by the condensing of oxidized hydrocarbons.

Trace gas: A gas that makes up less than 1% of the Earth's atmosphere.

Uptake Coefficient: The net loss of trace gas molecules proportionate to the total number of trace gas collisions with the surface. A unit-less number.

List of Figures and Tables

Figures

Schemes

Schematics

Tables

Chapter 1 - Introduction

1.1 Volatile Organic Compounds

The Earth's atmosphere consists largely of oxygen and nitrogen as well other trace gases such as oxidants and volatile organic compounds. The atmosphere also contains solids and liquids aerosol, which play major roles in atmospheric processes. These components of the atmosphere can undergo various reactions with one another, which can alter their impact on climate and health. For instance, these atmospheric reactions of trace gases with aerosols can alter the chemical properties of aerosols, serve as a source of tropospheric ozone, and affect the Earth's radiation budget. There is still a low-level of understanding in much of atmospheric chemistry especially regarding reaction involving aerosols (Usher et al., 2003). Studying the fate of atmospheric components provides a working model for atmospheric processes and gives a greater insight into the chemistry of the Earth's atmosphere.

An abundant and important component of the atmosphere is volatile organic compounds (VOC), which are emitted into the Earth's atmosphere through both biogenic and anthropogenic sources. Once in the atmosphere, these volatile organic compounds can react with oxidants forming new oxidized species through gas-phase processes. These gas-phase reactions contribute to the formation of tropospheric ozone, a major air pollutant that also acts as a greenhouse gas (Jacob, 2000). Volatile organic compounds can also undergo heterogeneous reactions with solid aerosol particulates. These reactions occur between compounds in the gas-phase and solid-phase which include the uptake of

volatile organic compounds on surfaces. These types of reactions have the ability to produce an organic layer on a solid, which can alter the chemical properties of the latter thereby affecting its fate in the atmosphere. For example, these modifications can affect cloud formation, solar radiation absorption and scattering, greenhouse gas concentrations, and other processes that greatly impact the Earth's climate (Kolb et al., 2010). Besides contributing to climate change, the presence of volatile organic compounds also have certain health impacts since they can enter the body through inhalation and skin exposure that can cause health problems such as lung cancer. They can also inflict oxidative damage to DNA while their reactions pose as a potential threat for the formation of toxic species (Shen et al., 2013).

Biogenic volatile organic compounds (BVOC) are the most prominent volatile organic compounds in the troposphere. They are emitted from ocean and terrestrial vegetation with an annual emission of nearly 1200 Tg yr^{-1} (Shen et al., 2013). Emissions are greatest in heavily wooded areas due to the expansive vegetation coverage. Land coverage maps such as in Figure 1 can be used to predict regions with greatest emissions. Tropical regions generally have the largest BVOC emissions due to a large presence of broad-leaf trees (Lathiere et al., 2006). Temperature, photosynthesis, leaf age, and other factors all contribute to emission levels (Guenther et al., 2006). Increasing temperature increases the chemical reactions within vegetation that produce BVOC, while simultaneously increasing vapor pressure of volatile compounds (Laothawornkitkul et al., 2009). Thus, an increase in temperature leads to greater BVOC emissions due to greater plant activity. Isoprene, a specific BVOC, is found to also be a thermal protectant for

leaves, and thus plants with greater emission values also have a higher heat tolerance, which may also explain why southern regions emit more isoprene and thus have higher BVOC emissions (Sharkey et al., 2008). BVOC emissions are also dependent on diurnal and nocturnal processes and with atmospheric concentrations dependent on the time of the day (Kim et al., 2010)
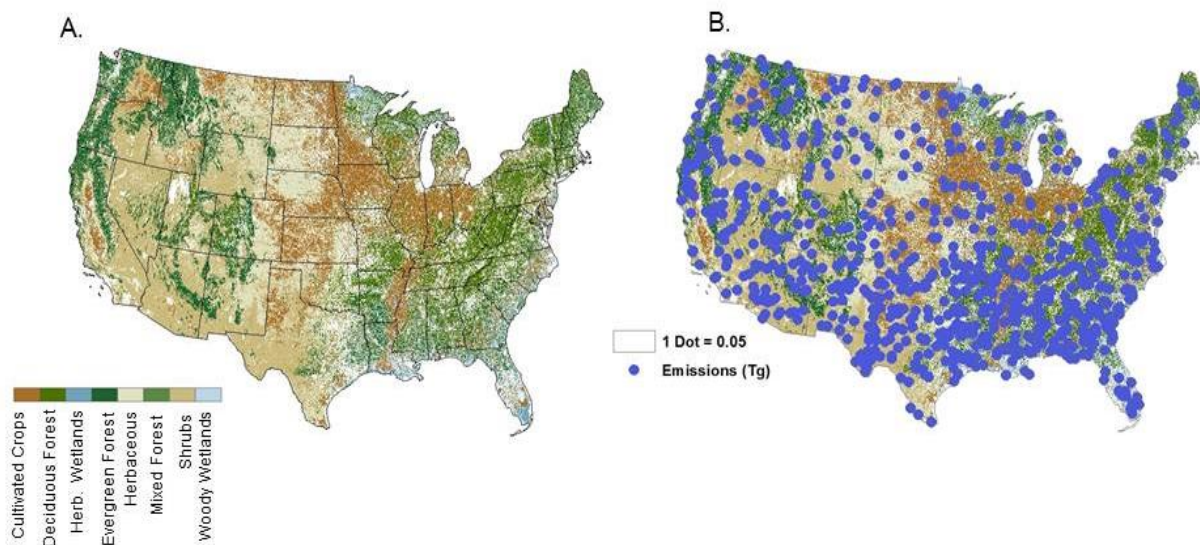
Figure 1: Distribution of United States of America biogenic volatile organic compound emissions from 2011. The map to the left (A.) is a land coverage map and the map to the right (B.) indicated the BVOC emissions per state in terms of dot density where 1 dot is approximately equal to 0.05 Tg. The National Emission Inventory (NEI) provides estimated air emissions of volatile organic compounds from biogenic sources in tons per year.

In the United States, southern regions have the greatest estimated BVOC emissions as seen in Figure 1 due to increased temperatures and longer growing seasons that account for a longer time span for BVOCS to be emitted from plants. Areas with the

largest forest coverage and minimal pasture land see the most significant BVOC

emissions. Densely populated regions with little foliar coverage have low emission rates.

1.2 Isoprene and Biogenic Volatile Organic Compounds

Biogenic volatile organic compounds are categorized into three main categories:

isoprene, various monoterpenes, and other BVOCs (Table 1). These compounds are all

emitted directly from vegetation at various emission levels. Isoprene is a conjugated

diene that consists of a four carbon chain with two double bonds and a methyl group (-

CH_3) attached at the secondary position. Monoterpenes are two isoprene units linked

together. Generally, the other BVOC category consists largely of oxygenated

monoterpenes and larger terpenes. The estimated annual emission level for each category

is listed in Table 1. It should be noted that the isoprene molecule has its own category due

to its large emission rates that are equivalent to half of total BVOC emissions. Even

though it has a strong presence in the atmosphere, there is still much unknown about

isoprene's fate in the atmosphere.
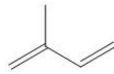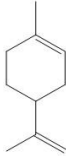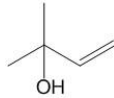
Structure	Type of BVOC	Annual Emissions (Tg yr^{-1})
	Isoprene	440 - 660
	Monoterpenes	32 - 127
	Other BVOCs	~ 520

Table 1: The annual emissions for isoprene, monoterpenes, and other BVOCs (Arneth et al., 2008) and (Laothawornkitkul et al. 2009). Limonene and 2-methyl-3-buten-2-ol are used for the structural examples for monoterpenes and other BVOCs, respectively.

As a hydrocarbon, isoprene is so abundant that its emission levels are second only to methane. As mentioned in Table 1, annual isoprene emissions are estimated to be 600 Tg yr^{-1}, which constitute half of total BVOC emissions (Muller et al., 2008). Estimated emissions are calculated using the Model of Emission of Gases and Aerosols from Nature (MEGAN), with variables including temperature, solar radiation, Leaf Area Index, and plant type (Guenther et al., 2006). The largest contributors to atmospheric isoprene concentration are regions densely populated with broadleaf trees and also shrubs in higher elevations (Guenther et al., 2006). However, factors including leaf age and weather conditions can alter emission levels as previously mentioned (Guenther et al., 2006). Currently, there are discrepancies between model estimates and field measurements of isoprene concentrations and these discrepancies are most prominent over forest canopies as shown in Figure 2 (Enami et al., 2012).

Our hypothesis that the clay minerals found in soil provides a reaction surface for the in-canopy isoprene, and this reaction can consume isoprene before it exits the forest canopy into the open atmosphere (Guenther et al., 2006). Clay minerals also exist as aerosols in the atmosphere, so interactions with isoprene are likely both through their existence in forest floors and as aerosols. Such processes are considered heterogeneous reactions, which involves the interaction of gas and solid phase materials. Future models require more vigorous algorithms that can predict changes in isoprene emissions due to physical and chemical environments (Guenther et al., 2006). Inclusion of heterogeneous reactions might explain overestimation of isoprene emission levels, especially over forest canopies. Another possible significant sink is the consumption of isoprene by microorganisms, which is another component found in soil (Cleveland et al., 1998).
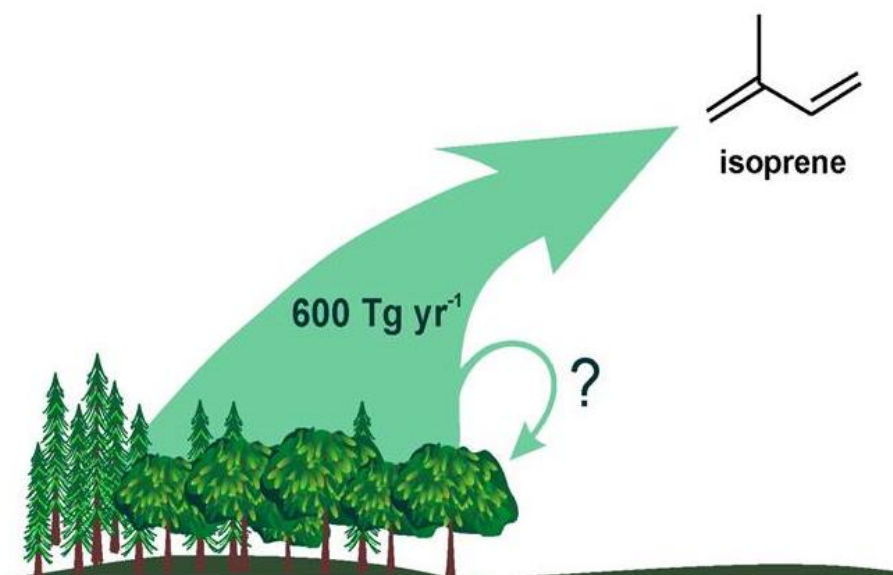
Figure 2. Isoprene is emitted into the Earth's atmosphere from vegetation at approximately 600 Tg per year. Discrepancies between field measurements and model estimations of isoprene suggest a missing isoprene sink, especially in forested regions.

It is important to first consider what is already known about isoprene's fate in the atmosphere. Once in the Earth's atmosphere, isoprene can be oxidized by hydroxyl radicals (OH), nitrate radical (NO_3), and ozone (O_3) (Carlton et al., 2009). Reactions driven by the hydroxyl radical and nitrate radical produces a set of volatile first generation products that can undergo further oxidation and form a multitude of semi volatile second generation products as shown in Scheme 1 (Carlton et al., 2009). Isoprene largely shapes the atmosphere's oxidation chemistry due to its natural abundancy and predisposition to undergo oxidation due to its two double bonds (Paulot et al., 2009). Nearly one-third of isoprene is predicted to undergo oxidation by the hydroxyl radical (OH) (Henze et al., 2006). These oxidized products are less volatile and therefore are likely to form secondary organic aerosols.
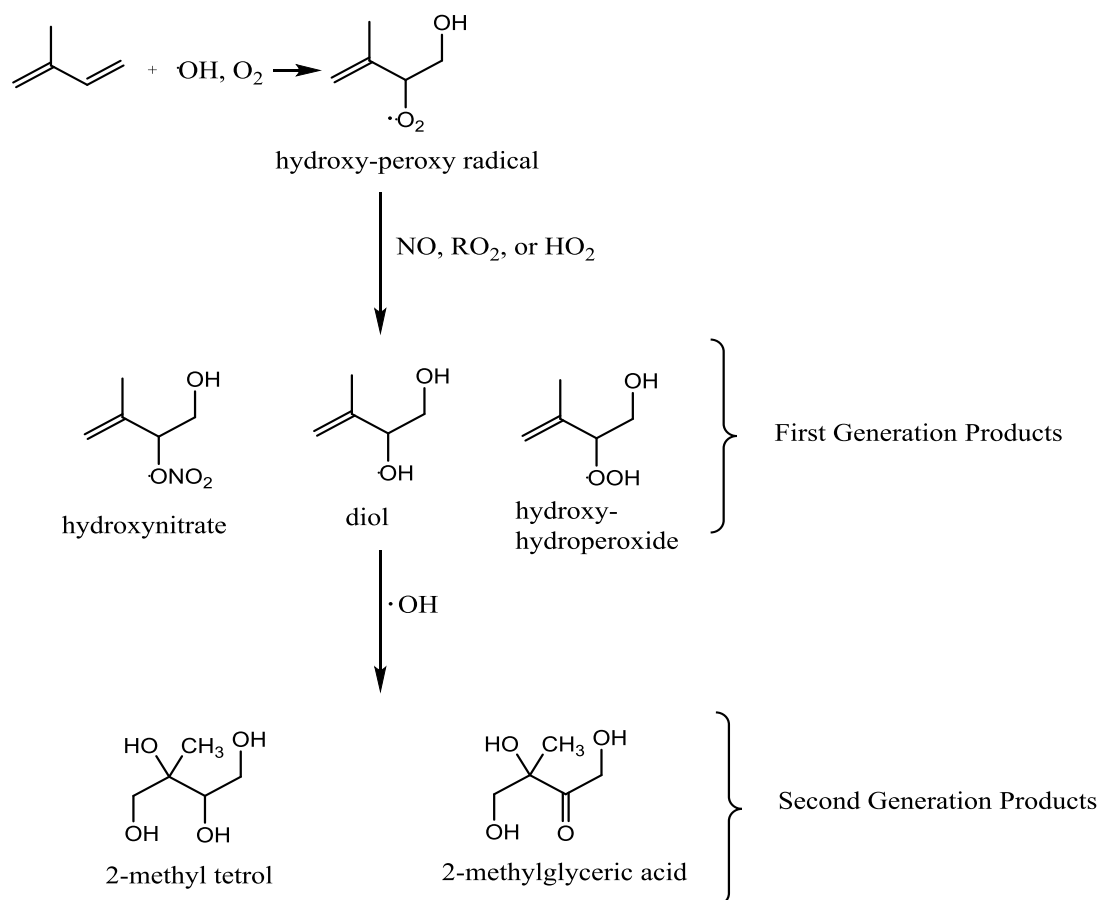
Scheme 1: The OH radical initiated reactions of isoprene that produces first generation products followed by additional reactions that produce second generation products.

It has been suggested that under low NO_x conditions, isoprene recycles the hydroxyl radical, which can lead to further oxidation of other isoprene molecules (Archibald et al., 2010). Furthermore, one contributor to the concentration of hydroxyl radicals is the ozonolysis of isoprene (Malkin et al., 2010). The hydroxyl radical is thought to be an atmospheric cleanser that contributes to the degradation of BVOCs being largely responsible for their removal from the atmosphere during the day (Archibald et al., 2010). The emissions of isoprene can influence hydroxyl levels

especially over forest canopies and thus indirectly affect atmospheric oxidation processes (Malkin et al., 2010). The reaction of isoprene with hydroxyl radicals in the presence of NO_x can both contribute to tropospheric ozone levels and act as a sink for NO_x by conversion of NO to NO_2, which forms ozone upon photolysis (Lockwood et al., 2010). The contribution to ozone level depends on the presence of NO_x. Low levels of NO_x will force isoprene to react with ozone, thereby decreasing ozone levels (Sanderson et al., 2003). Therefore, it is suggested that isoprene can largely dictate oxidant levels in the Earth's atmosphere through its gas-phase reactions, showing that isoprene does largely shape the chemistry of the atmosphere.

Previously, the uptake of isoprene on water surface has been studied and it was found the isoprene oxidizes on the surface of a pH < 4 water. The uptake coefficient for the oxidation of isoprene on aqueous $FeCl_2$ solution for this particular experiment was found to be in the range of 10^{-3} to 10^{-4} range (Enami et al. 2014). Prior studies have shown that the uptake of isoprene on water at pH < 3 (as opposed to acidic aqueous solutions with $FeCl_2$ present) to be in the range of 10^{-6}-10^{-7} and to be in the range of 10^{-6} for acidic aerosols such as sulfuric acid (H_2SO_4) (Enami et al. 2012). Therefore reactive uptake of isoprene on mildly acidic surfaces has been shown as a viable pathway for the consumption of isoprene.

Monoterpenes, as mentioned previously, can undergo similar oxidation processes in the atmosphere. These oxidized monoterpene products are less volatile and can condense to form secondary organic aerosol (SOA). These are a class of atmospheric

aerosols which consists of particles that are suspended in the air and are formed when oxidized hydrocarbons condense. There is still a large uncertainty associated with SOA production levels. The global production of SOA from all biogenic origins is estimated to be between 10 – 30 Tg yr^{-1}(D'Andrea et al., 2013). However, the SOA estimation is much debated due to the large uncertainty, as shown by the variability in Table 2, in how much individual BVOCs contribute to the total yield. This number could be much higher once all BVOC sources of SOA become better defined. The estimated annual SOA contributions from isoprene and terpenes are listed in Table 2.

Source of SOA	Estimated contribution (Tg yr^{-1})
Isoprene	2- 30
Terpenes	19.1
Total non-isoprene BVOC	12 - 70

Table 2: Estimated annual contributions to SOA yield from isoprene and terpenes (Carlton et al., 2009) (Kanakidou et al., 2008).

Biogenic secondary organic aerosols can serve as cloud condensation nuclei (CCN) which are fine particles that act as a surface for water to condense upon and promote cloud formation. In the Amazon, the submicrometer particles that contribute most to cloud condensation nuclei are composed largely of secondary organic aerosol originating from oxidized BVOCs (Posch et al., 2010). Secondary organic aerosol can also promote ice nucleation, which occurs below temperatures of 238 K (-35°C) (Wang et al., 2012). Ice nucleation is the process in which a particle acts as the nucleus for the formation of ice in the atmosphere, and can affect cloud properties. Pure SOA may act as

ice nuclei, but studies so far have proven that they are an unlikely source of ice nucleation (Prenni et al., 2009). However, the formation of secondary organic coatings on aerosols may still alter ice nucleation abilities. Secondary organic aerosol coatings on particles that do serve as ice nuclei have shown to inhibit ice nucleation abilities (Mohler et al., 2008). The presence of SOA on particle surfaces, such as mineral dust, can modify the particle's composition which can alter its chemical properties. Therefore, SOA coatings on particles can limit their ability to act as an ice nucleus and change the number of particles which promote ice nucleation thus altering the radiative properties of clouds (Prenni et al., 2009).

Oxidized isoprene products were once thought to *not* contribute to SOA formation due to the volatile nature of their low molecular weights. However, field evidence has been reported that supports isoprene SOA formation through second generation oxidized compounds including the isoprene tetrol (Carlton et al., 2009). Currently, the isoprene contribution to SOA is estimated to be between 2 and 30 Tg yr^{-1} (Table 2), however these values may be much larger (Carlton et al., 2009). Isoprene as a precursor to secondary organic aerosol would greatly increase the estimated SOA concentrations and may provide reconciliation between low SOA predictions and observations (Henze et al., 2006). It is now believed isoprene can contribute to SOA yield through the second generation oxidized produces, the 2-methyl tetrols. Aerosol samples from Brazil have been analyzed and found to contain the isomers of the 2-methyl tetrol: 2-methylthreitol and 2-methylerythritol (Claeys et al., 2004). 2-Methylthreitol and 2-methylerythritol have the isoprene skeleton as shown is Figure 3 and are known as the 2-methyltetrols (Carlton

et al., 2009). Claeys et al. proposed that it was a reasonable assumption that these compounds came from the photooxidation of isoprene (2004). Other field experiments also detected 2-methyltetrols in aerosol samples from boreal forests in Finland (Kourtchev et al., 2005).

| Isoprene | 2-Methylthreitol | 2-methylerythritol |
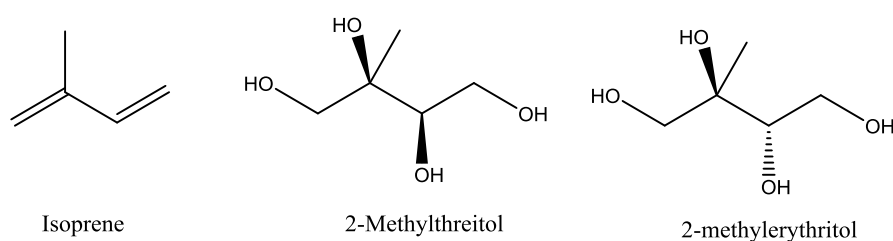
Figure 3: The structures of isoprene, 2-methylthreitol, and 2-methylerythritol. Isoprene is suggested to contribute to secondary organic aerosols through the 2-methyl tetrol isomers.

The finding of 2-methyltetrols in aerosol samples has supported the case for isoprene as a precursor to secondary organic aerosol. Recent laboratory studies have also confirmed these findings. Aerosol formation from isoprene oxidation has been observed at high concentrations of NO_x and most likely results from the tetra-substituted compounds, 2-methyltetrol (Kroll et al., 200
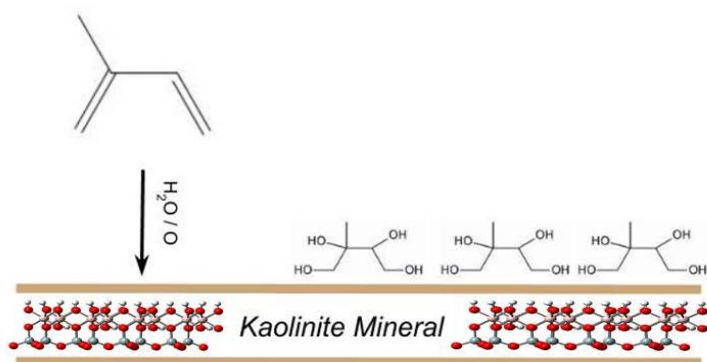
Figure 4: Our hypothesis is that the heterogeneous reaction between isoprene and the kaolinite mineral produces the 2-methyl tetrol isomers that is suspected to form as a layer on the kaolinite surface.

We hypothesize that the heterogeneous reaction of isoprene and kaolinite, a type of clay mineral found in soil and as an aerosol, will produce the isoprene tetrol (Figure 4). Due to the less volatile nature of the isoprene tetrol, it is suspected that the tetrol will remained adsorbed onto the surface of the mineral while interacting with surface oxygens. An isoprene tetrol layer could then alter the chemical properties of the mineral dust and lead to changes in its atmospheric processes such as ice nucleation abilities and radiative forcing.
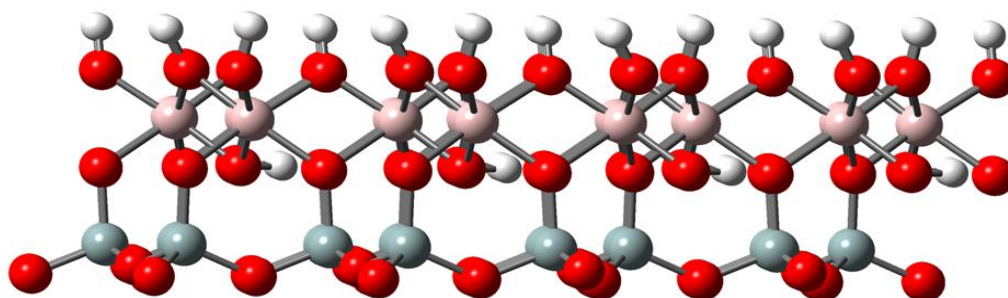
Figure 5. The structure of kaolinite, a clay mineral, which is part of the aluminum silicates. Kaolinite has surface oxygens which can act as redox sites as well as water embedded throughout the structure which can be used in acid catalyzed hydrolysis.

Kaolinite is a clay mineral and is part of the aluminum silicates (Figure 5). On the surface of the kaolinite are oxygens that can act as reduction/oxidation (redox) sites. Embedded throughout the kaolinite is water even under relatively dry conditions that can contribute to acid catalyzed hydrolysis of biogenic volatile organic aerosol. Previous studies at Drew University has shown that limonene, another BVOC, can react with kaolinite following two different processes as shown in Scheme 2 (M. Lederer, 2016). We propose that the heterogeneous reaction of isoprene and kaolinite will undergo a similar process. These processes include the acid catalyzed reaction to form gaseous 2-

methyl-3-buten-2-ol (MBO) and also the formation of an epoxide intermediate that will

eventually form the 2-methyl tetrol (Scheme 3).
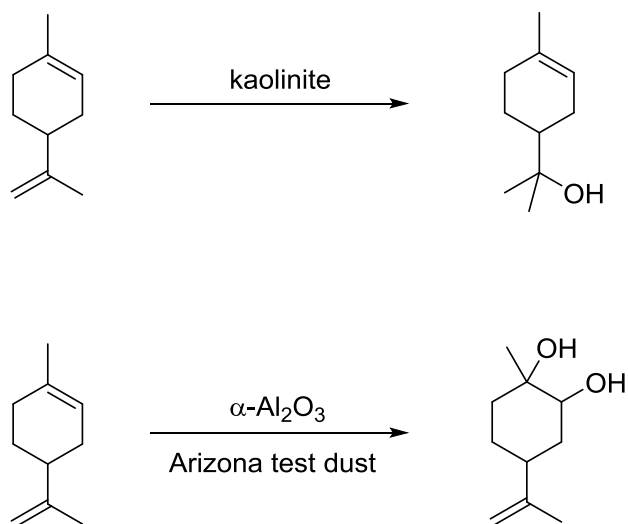
Scheme 2. The reaction of limonene with kaolinite and Arizona test dust produced the oxidized products as shown above through either acid catalysis or an epoxide intermediate. These reactions prompted further research into the reactive uptake of various BVOCs and clay minerals.
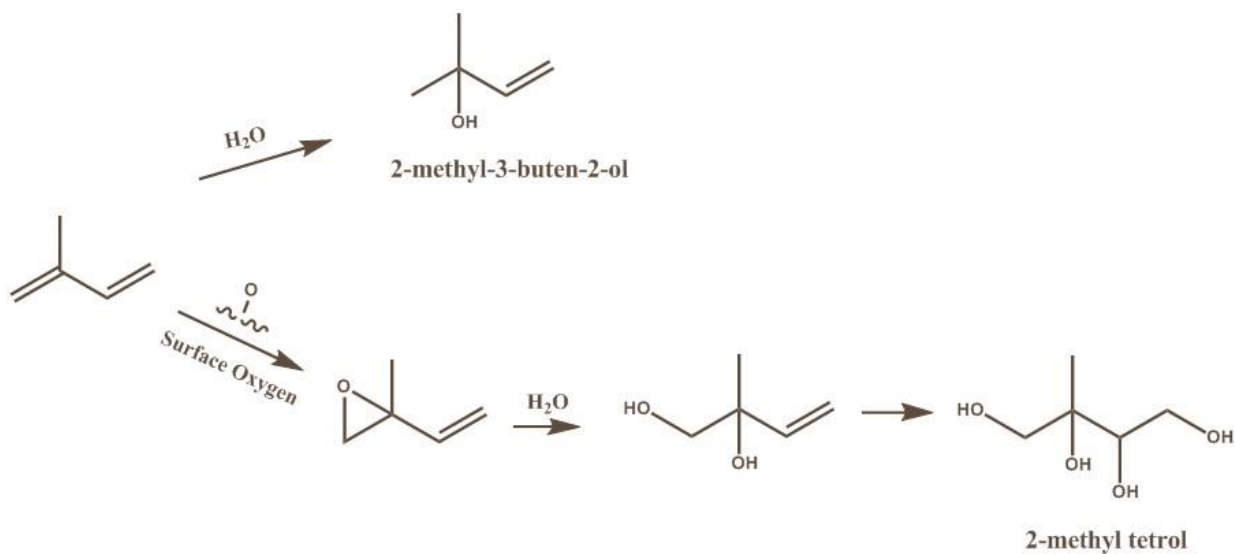
Scheme 3. The proposed mechanism for isoprene and kaolinite which can either undergo acid catalyzed hydrolysis to form the 2-methyl3-buten-2-ol or form an epoxide intermediate which will ultimately form the 2-methyl tetrol.

1.3 Reactive Uptake on Mineral Dust

   Clay minerals are ubiquitous in the atmosphere as aerosols and are found as part of the composition of soil so interactions with isoprene are likely. Several minerals are found in mineral dust aerosol, including quartz (SiO_2), carbonates ($CaCO_3$), and aluminum silicate clays such as kaolinite ($Al_2Si_2O_5(OH)_4$) (Usher et al., 2003). The estimated emissions for mineral dust ranges from 1000 to 2150 Tg yr^{-1}. Dust particles are picked up by wind currents in arid regions and have a long distribution range. Most of the mineral dust that is in the atmosphere originates from one central location with little activity outside of this region (Todd et al., 2008). This area spans the west coast of North Africa, the Middle East, and also Central and South Asia (Zhang et al., 2003). Further studies have shown that mineral dusts from these sources are wide spread throughout the world. Satellite sampling found that African dust events affect much of the southern portion of the United States, and one study in particular found that dust from Africa dominated in Miami during summer aerosol sampling, (Prospero, 1999). Mineral dust itself plays an important role in atmospheric chemistry including direct and indirect climate effects. Mineral dust has the capability of absorbing or scattering radiation, act as ice nuclei, alter trace gas concentrations by adsorbing organic compounds, and can also be a key component in heterogeneous reactions as illustrated in Figure 6 (Kolb et al., 2010).
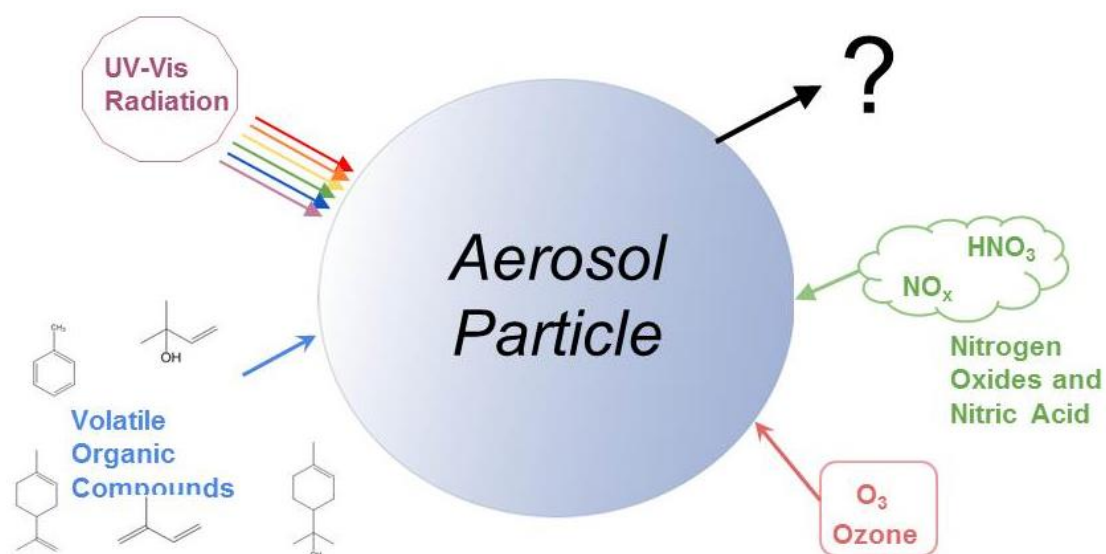
Figure 6. Mineral dust aerosols are involved in many processes in the atmosphere including absorbing/scattering radiation, adsorbing volatile organic compounds, and reactions with oxidants such as ozone.

Mineral dust is a relevant surface for the uptake of biogenic volatile organic compounds. The reactive uptake of trace gases results from gas molecules colliding with surfaces and adsorbing, which means to adhere to a surface and forming a film, which also includes reacting with the surface itself (Kolb et al., 2010). Previous studies on the BVOC limonene and clay minerals have shown promising reactive uptake by the reactions (M. Lederer, 2016). As a result, the finding of these studies prompted further research into the reactions of other BVOCs and clay minerals. Heterogeneous reaction and therefore the reactive uptake of volatile organic compounds can be defined by kinetic parameters that include uptake coefficients (γ). The uptake coefficient is a unit-less number that defines the net loss of trace gas molecules proportionate to the total number of trace gas collisions with the surface under study with a maximum uptake coefficient of

1 and provide context for atmospheric relevancy of a heterogeneous reaction (Shen et al.,

2013). Several factors that can alter the magnitude of an uptake coefficient include

relative humidity and temperature. Therefore it is beneficial for reactive uptake studies to

be performed under atmospherically relevant conditions.

Several lab methods exist for measuring the experimental uptake and reaction of

gases with surfaces. This paper will examine the coated wall flow tube reactor, referred to

as the horizontal laminar flow reactor, as a system designed to measure uptake kinetics.

The general process of the laminar flow reactor includes passing a trace gas under study

through a tube coated with the solid of interest (such as mineral dust). Changes in trace

gas concentration are monitored downstream from the injection point often by a mass

spectrometer or other spectroscopic means. In most cases, the trace gas is introduced into

the system through a movable injector. This allows for variations in time of exposure that

permits for the measurement pseudo-first order rate constants while a fixed distance

allows for measurements regarding surface saturation (Kolb et al., 2010). The laminar

flow reactor introduces radial diffusion that needs to be corrected for in uptake

coefficient calculations. Several methods exist that account for tube geometry and

diffusion effects. This study uses the laminar flow reactor in conjunction with the

mathematical process developed by Knopf, Poschl, and Shiraiwa (2015), to calculate the

uptake coefficient for the heterogeneous reaction of isoprene and kaolinite.

A horizontal laminar flow reactor was constructed for the use of this study.

Calibration and corrections will be discussed and necessary flow parameters will be

reviewed. The laminar flow reactor is used to monitor the reaction between isoprene and kaolinite and measure reactive uptake. With the uptake coefficient, the relevancy of the heterogeneous reaction between isoprene and kaolinite can be determined. An uptake coefficient that is larger in magnitude will indicate that the reactive uptake of isoprene on minerals is a relevant reaction in atmosphere. Additionally, samples from this reaction were analyzed using Diffuse Reflectance Infrared Fourier Transform Spectroscopy (DRIFTS) and Gas Chromatography-Mass Spectroscopy to identify surface adsorbed products from this reaction. Preliminary studies suggest that the heterogeneous reaction of isoprene and kaolinite produces 2-methyl tetrol (isoprene tetrol) however the stability of the compound is still under investigation (Scheme 4).
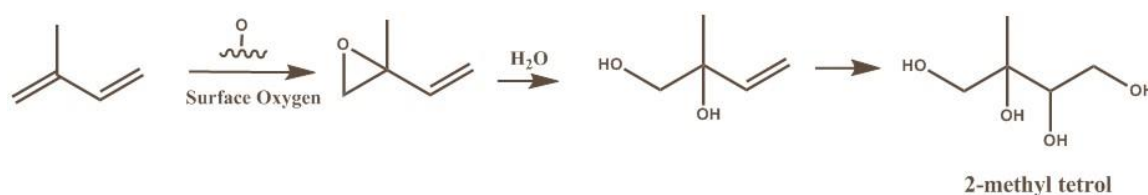
Scheme 4. It is proposed that the heterogeneous reaction of isoprene and kaolinite will follow a redox reaction with surface oxygens to form an epoxide intermediates which are then attacked by water to form the 2-methyl tetrol.

Chapter 2 – Laminar Flow Reactor

2.1 Design of the Laminar Flow Reactor

Initially, this study aimed to detect the formation of gaseous products from heterogeneous reactions. Previous methods were inadequate to monitor gaseous product formation because only products adsorbed to the aerosol substrate surfaces were measured instead of gaseous species. This prompted the construction of a horizontal laminar flow reactor coupled to a gas-analysis mass spectrometer. The horizontal laminar flow reactor allows for controlled mixing of isoprene and kaolinite while the mass spectrometer can detect gases down to parts per billion (ppb). It was found that no gaseous products were formed during the heterogeneous reaction of isoprene and kaolinite however the flow reactor was still well suited to monitor the kinetics for this reaction. The flow reactor is also more advantageous in monitoring changes in isoprene concentration when compared to previous methods that included the use of Fourier Transform Infrared (FTIR) gas cell analysis due to residence times. The residence time is greater for the FTIR gas cell with a 10 meter path length because of its increased volume and slower flow rate (~300 SCCM). This larger residence time increases the amount of time required for the isoprene concentration to stabilize and decreases the sensitivity to changes in concentration on the order of minutes which create imprecise kinetic measurements. The flow reactor has much shorter residence time, and can detect changes in concentration on the order of seconds. Therefore, the problems of other methods are bypassed and more accurate kinetic measurements are achieved.
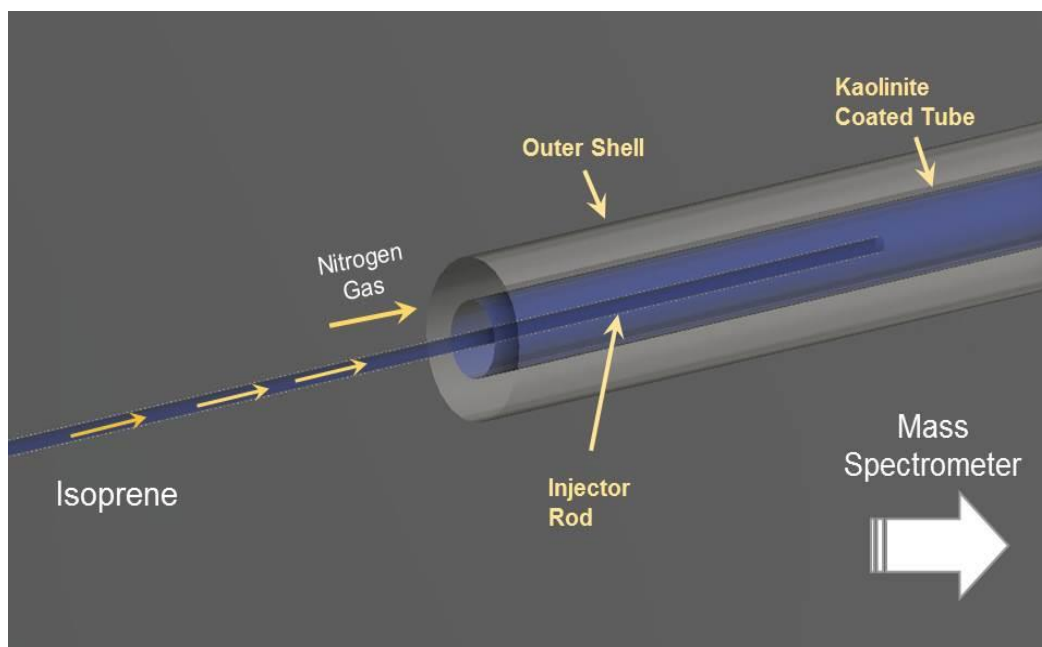
Figure 7: The three main components of the laminar flow reactor are displayed. The outer shell houses the entire system, the inner tube is coated with kaolinite, and isoprene enters the flow reactor through the injector rod while nitrogen gas continuously is pumped directly into the flow reactor. At the end of the flow reactor is an HPR-20 gas analysis mass spectrometer.

2.2 Laminar flow reactor and experimental design

The laminar flow reactor as displayed in Figure 7 consists of a 147-cm long water-jacketed flow tube, which holds a 122-cm long glass tube with an inner diameter of 2.5-cm that is entirely coated with mineral slurries, and a centered, movable injector rod introduces the isoprene into the reactor moving through the slurry-coated glass tube. When the injector rod is fully inserted, isoprene does not interact with the mineral coated insert tube and the mass spectrometer measures the initial concentration of isoprene, $[Iso]_{t=0}$. Once the injector rod is pulled back, isoprene is introduced into the entire system and it interacts with the mineral coated insert tube, $[Iso]_{t=s}$. The diameters, volume, and surface area of each flow reactor component (Figure 8) are given in Table 3.

Component	Fig. 7 Label	Inner Diameter (cm)	Length (cm)	Volume (cm³)	Surface Area (cm^2)
N₂ inlet	a.	0.11			
injector rod	b.	0.15			
insert tube	c.	2.48	122	589	951
flow tube	d.	3.6	147	1496	1663

Table 3. Flow reactor parameters including inner diameter, length, volume, and surface area of kaolinite coating. Labels correspond to Figure 7.
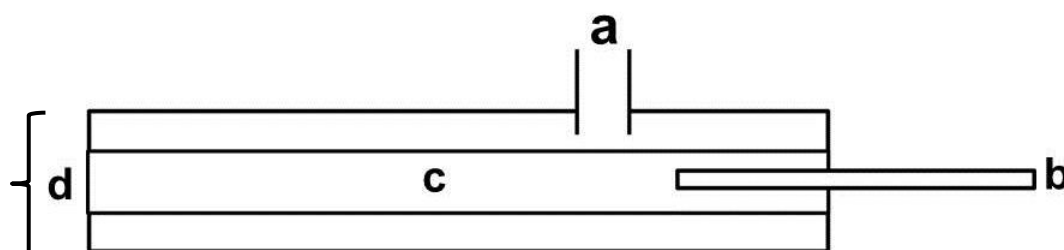
Figure 8. The labeled components of the flow reactor where a corresponds to the N_2 inlet, b is the injector rod, c is the insert tube, and d is the flow tube.

A N_2 cylinder supplies the flow reactor with a constant stream of nitrogen gas as shown in Schematic 1. This supply is separated into two sections before reaching the flow reactor to introduce both dry and wet flows into the system. One section goes straight to the flow reactor and supplies a dry nitrogen gas flow. The other section, which has the ability to be diverted, is connected to a water bubbler. The two sections are rejoined and the resulting flow runs through a length of tubing to ensure mixing before being introduced into the system. This allows for experiments using dry flows only and also flows with variations in humidity. Nitrogen gas is also directed into an isoprene bubbler, with diversion possible to exclude isoprene from the flow. The nitrogen acts as a carrier gas and introduces isoprene into the flow reactor system through the movable

injector rod. Master flow controllers (MFC) determine the flow rates and are used to

manipulate the concentration of isoprene.
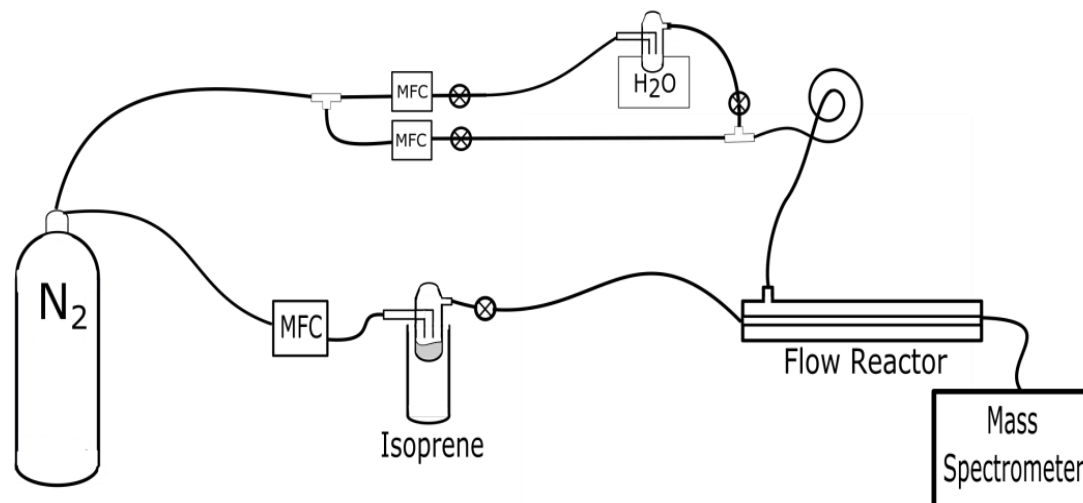
Schematic 1: Laminar flow reactor schematic. Nitrogen flows through the flow reactor (bulk flow) and can pass through a water bubbler to introduce humidity into the system or can be bypassed for a dry flow. A trace amount of nitrogen flows through isoprene in a bubbler which then introduces isoprene into the flow reactor. The isoprene exits the flow reactor and a section is sent to the mass spectrometer.

2.3 Flow pattern
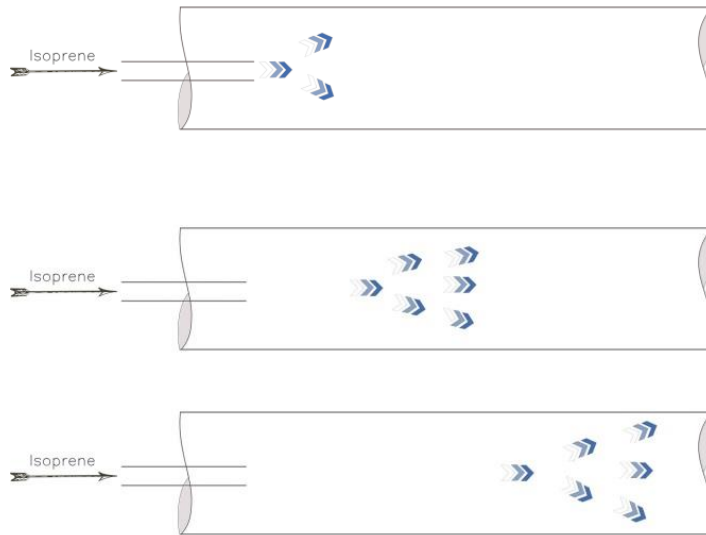
Figure 9a. Progression of a laminar flow. The arrows indicate that the flow is continuous and moves in ordered layers without disturbances.
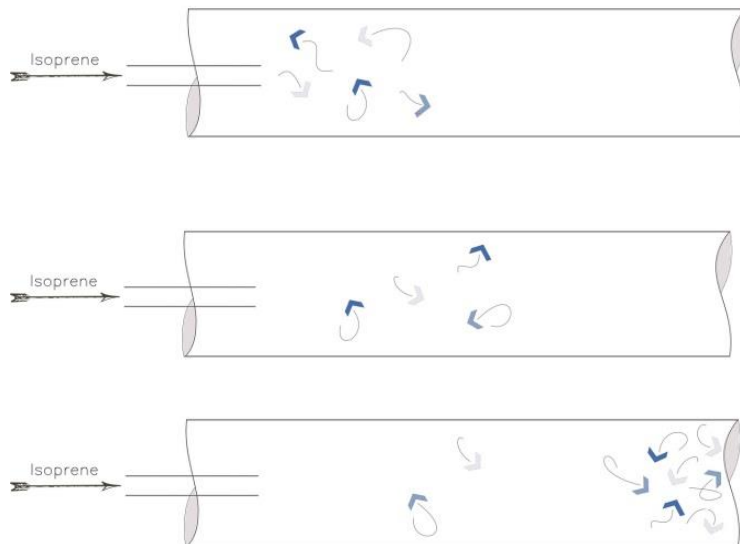
Figure 9b. Progression of a turbulent flow. Arrows indicates that the flow can have any direction, and different air particles can have different speeds simultaneously.

The resulting flow pattern was modeled using the Reynolds number (Re), which

is a unit-less number used in fluid dynamics to predict the flow pattern in a given system.

It is the ratio of inertial forces to viscous forces and determines if a flow is laminar or turbulent. An inertial force is defined as resistance to changes in momentum and is characterized by the mass of the particles. The friction between the layers of the flow is defined as the viscous force. In laminar flow, the viscous forces are larger than the inertial forces and the flow remains consistent and smooth. In turbulent flow, the inertial forces dominate, and the flow turns chaotic and sporadic as swirls and irregular flow patterns are produced. Laminar flow is depicted by stacked arrows in Figures 9a and turbulent flow is depicted by swirls in Figures 9b. A Reynolds number of less than 1000 indicates that the flow is laminar, and in our system, a low Reynolds flow number is desired. Due to the consistent nature of the laminar flow, we can predict the collision of particles with the flow reactor walls and measure the residence time, which is the time a particle spends in a system, or in our process, the time it takes for isoprene to reach the mass spectrometer once it enters the flow reactor.

The Reynolds number is calculated by Equation 1. The density of the fluid and the dynamic viscosity is described as ϱ and μ with values for air (bulk flow) at 20°C of 1.2041 kg m^{-3} and 1.81x10^{-5} kg m^{-1} s^{-1} respectively. V and D are the flow velocity (m/s) and diameter (meters) of the tube the fluid moves through.

Equation 1: $$Re = \frac{\varrho VD}{\mu}$$

The maximum flow rate that can be used to still maintain a laminar flow within the flow reactor itself is approximately 17,000 standard cubic centimeters per minute (SCCM).

Due to the tubular design of the laminar flow reactor, radial diffusion needs to be accounted for in reactive uptake coefficient calculations. Diffusion is the dispersion of

molecules, such as isoprene, in a system due to random motion from a highly

concentrated region to a region with low concentration. In a hollow cylinder, like the one

employed in the flow reactor, diffusion is radial in nature and concentration becomes a

function of radius and time (Crank, 1975). In these laminar conditions, isoprene will

travel faster in the center of the flow tube and slow down near the walls thus creating a

concentration gradient that is dependent on the flow velocity, flow reactor specifications,

and diffusion as shown in Figure 10 (Knopf et al., 2015). Diffusion and the

corresponding concentration gradient need to be corrected for in uptake calculations. We

used the recently published KPS method to calculate the uptake coefficient of isoprene

and kaolinite. There are six assumptions made in the KPS calculations that are as

follows: 1) isoprene is a trace gas in the bulk flow of nitrogen gas; 2) the flow in the flow

reactor remains laminar i.e., a Reynold's number if less than 1000; 3) the temperature and

viscosity of the gas is homogeneous; 4) bulk flow velocity dominates over axial diffusion

velocity; 5) the uptake of isoprene is small compared to its concentration; and 6) there are

no gas-phase reactions that impact the concentration of isoprene (Knopf et al., 2015).
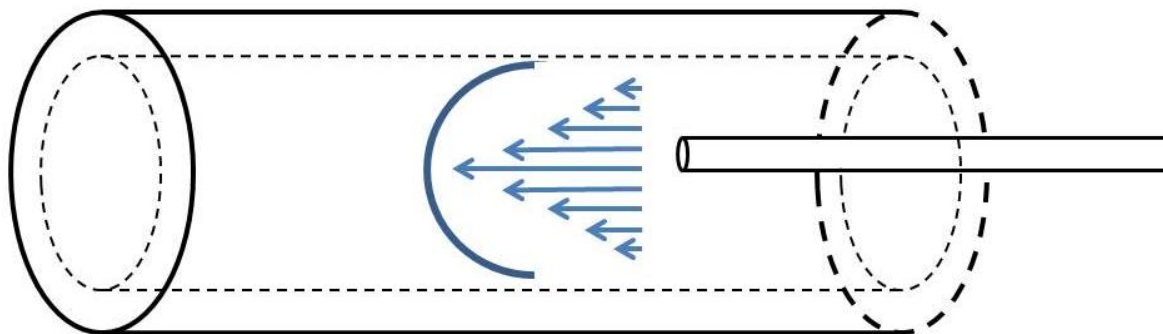
Figure 10. Due to uptake to kaolinite on the flow reactor walls, isoprene molecules are lost to uptake which creates a concentration gradient dependent.

To begin the KPS calculations, the Péclet number (Pe) needs to be calculated. The Péclet number is another dimensionless number that describes the relationship between mass transport by advection to mass transport by diffusion. Advection is the bulk movement of particles and diffusion is the movement of particles from high concentration to low concentration regions. For Péclet numbers less than one, mass transport by diffusion dominates (Huysmans et al., 2004). The Péclet number is given in Equation 2, where D_{tube} is the tube diameter, v_g is flow velocity, and D_g is the gas-phase diffusion coefficient of isoprene. The gas-phase diffusion coefficient can be calculated by dividing the diffusivity of isoprene (73 Torr cm^2 s^{-1}) by atmospheric pressure of 760 torr (Tang et al., 2015). For Péclet numbers greater than 10, mass transport by advection dominates and axial diffusion can be ignored. The differences between radial diffusion and axial

diffusion are displayed in Figure 11. At fast flow rates (8500 SCCM), the Péclet number

for the flow reactor is 540, meaning assumption 4 is valid.

Equation 2:
$$Pe = \frac{D_{tube} * V_g}{D_g}$$
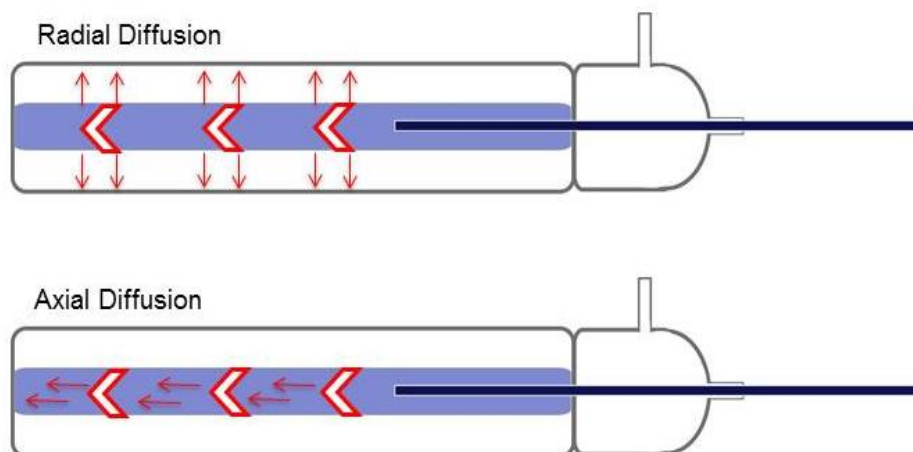
Figure 11: The depiction of radial and axial diffusion in the laminar flow reactor.

Isoprene concentration in the flow reactor is largest in the center of the tube and

disperses as the radial distance increases. To calculate the reactive uptake coefficient, the

concentration of isoprene within one mean free path (λ_x) of the surface, [isoprene]$_s$, needs

to first be determined. The mean free path (Figure 12) is the average distance that a gas

molecule travels between collisions and can be calculated using the kinetic theory of

gases, $\lambda_x = 3D_g/\omega_x$, where ω_x is the thermal molecular velocity of isoprene. The thermal

molecular velocity can be determined by calculating $V_{rms} = \sqrt{\frac{8RT}{\pi MW}}$, where R is the gas

constant (8.314 J mol^{-1} K^{-1}), T is temperature, and MW is the molar mass of isoprene in

kg mol^{-1} which results in units of m/s.
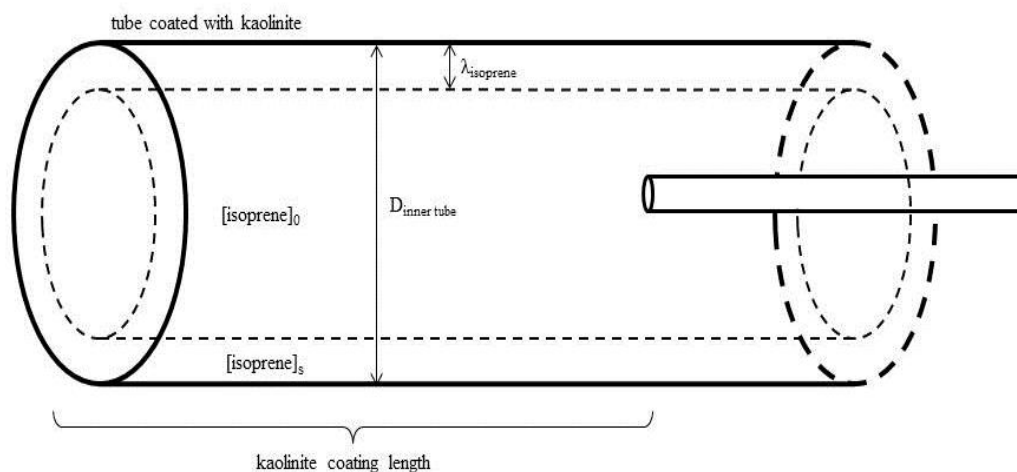
Figure 12. Illustration of flow reactor parameters as discussed: inner diameter of inserted tube ($D_{inner\ tube}$), average initial concentration of isoprene ([isoprene]$_0$), isoprene concentration within one mean free path of surface ([isoprene]$_s$), and one mean free path from surface of kaolinite coating ($\lambda_{isoprene}$). The kaolinite coating length refers to the portion of the coated tube that is exposed to isoprene during the reaction.

At the initial point of gas injection, the gas enters a region commonly referred to as the entrance region which is the portion of the tube that is undefined until laminar flow is fully developed. The point at which laminar flow is established in the flow reactor can be approximated by L=0.035*D_{tube} *Re (Knopf et al., 2015). In our experiments, laminar flow is achieved at 40 cm into the flow reactor. Further information about the flow upon entry can be determined by calculating the dimensionless axial distance (z*) which is calculated by normalizing the axial distance (z) of the coated tube that is exposed to isoprene. The portion of the kaolinite coated tube that is exposed to isoprene during the experiment is 112.08 cm. The equation for dimensionless axial distance is given in

Equation 3 where Q is the volumetric flow rate in SCCM. For fast flow rates, the dimensionless axial distance is 0.12.

Equation 3 $$z^* = z * \frac{\pi}{2} * \frac{D_g}{Q}$$

The Knudsen number is dimensionless number that describes the flow regime of cylindrical geometries such as a flow reactor as the ratio of the mean free path length to radius of the tube. It can be calculated using the diameter of the coated tube as given in Equation 4 (Knopf et al., 2015).

Equation 4. $$Kn = \frac{2\lambda_x}{D_{tube}}$$

At Knudsen numbers less than 1, the gas is a continuum fluid that follows continuum mechanics that models matter as continuously dispersed with no empty spaces. For our fast laminar flow reactor, the Knudsen number was found to be $7\text{x}10^{-6}$, which indicates that the system follows continuum mechanics. All calculations and parameters can be found in Table 4 and are compared to other flow tube experiments. We expected parameters similar in magnitude to the BSA and O_3 values due to similarities in the slow uptake of both reactions.

Parameter	Fast Flow Reactor	Slow Flow Reactor	OH + levoglucosan (Knopf et al., 2015)	NO$_3$ + abietic acid (Knopf et al., 2015)	O$_3$ + BSA (Knopf et al., 2015)
Table 4					
Diameter Flow Tube (m)	0.032	0.032	-	-	-
Diameter Inner Tube (cm)	2.48	2.48	1.77	1.758	0.8
Diameter Inner Tube (m)	0.025	0.025	0.018	.018	0.008
Outer Diameter Inner Tube (cm)	2.8	2.8	-	-	-
Kaolinite Length (m)	1.12	1.12	-	-	-
Volume Flow Tube (cm)	753		-	-	-
Volumetric flow rate (SCCM)	7100	1200	-	-	-
Velocity (m/s)	0.175	0.03	28.74	9.14	0.302
Re	380	64	22.5	4.2	190.50
L (cm)	0.330	0.056	3.6	10	50
D$_g$ (Torr cm^2/s at 298K)	0.0961	0.0961	188.22	95.72	0.1267
Pe$_x$	451	76	28.71	16.79	190.50
z*	0.143	0.846	0.15	0.68	0.66
ω (cm/s)	3.04E+04	3.04E+04	6.04E+4	3.19E+4	3.6E+4
λ$_x$ (cm)	2.99E-04	9.47E-6	9.35E-3	9.00E-3	1.1E-5
Kn	2.41E-04	7.64E-6	0.01	0.01	2.8E-5
[X]$_{g,0}$ (Molecules/cm^3)	3.32E+15	3.32E+15	1.71E+9	7.3E+10	2.7E+12
t (s)	6.36	37.6	0.00126	0.01094	1.657
N^{eff}	4.27	3.77	-	-	-

2.4 Calibrating the HPR-20 Mass Spectrometer

Coupled to the flow reactor is a Hiden HPR-20 gas-analysis mass spectrometer. In a mass spectrometer, molecules lose electrons to form ions. During ionization, molecules can break apart to form what are known as fragments. These ions proceed to an analyzer where they are detected based on their mass to charge ratio. The abundancies of each ion at the detector is displayed as relative ion intensity.

The mass spectrum of isoprene was recorded using the HPR-20 quadropole mass spectrometer and is displayed in Figure 13. The mass spectrometer has a dual Faraday Cup/Secondary Electron Multiplier Detector (SEM). The electron multiple generates secondary electrons by collisions of ions with the surface which creates a cascade effect that increases gain by a thousandfold. The SEM detector was used in all data collection processes with a mass range was from 30 to 100 amu. The default Global Environment was used with an electron energy for 70 volts. Some of the fragmentation pattern is depicted in the mass spectrum provided. The peak at 68 m/z represents the molecular ion and results from the loss of an electron from the isoprene molecule. This peak corresponds to the molecule weight. A peak at 53 m/z results from the loss of a methyl (CH_3) radical, and a peak at 39 m/zz corresponds to an additional loss of methylene (CH_2).

Mass Spectrum of Isoprene
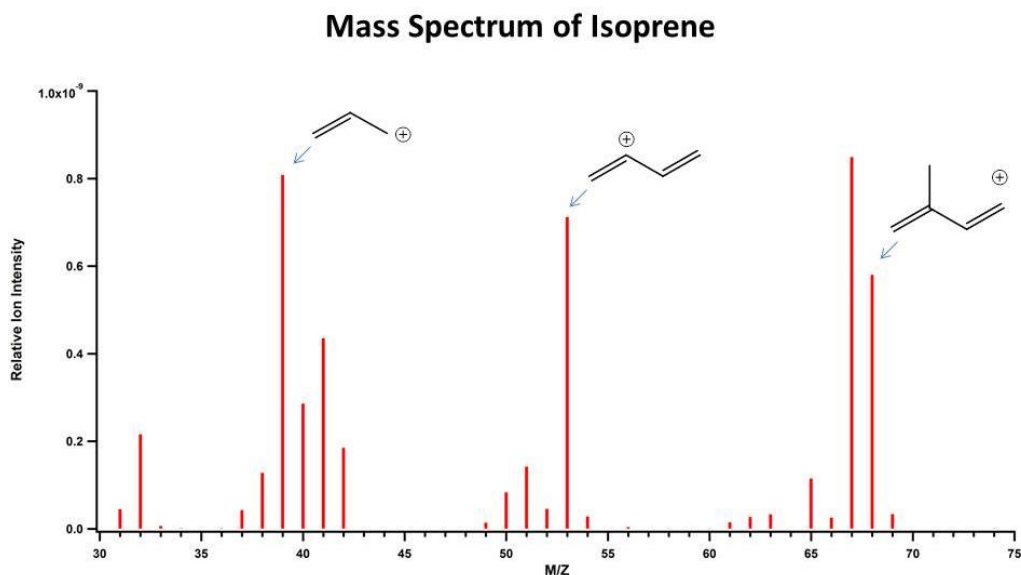
Figure 13. The mass spectrum of isoprene as recorded by a Hiden HPR-20 mass spectrometer. A brief depiction of the fragmentation pattern has been provided. The peak at 68 m/z corresponds to the molecule ion of isoprene.

To convert from ion intensity to concentration of isoprene, the mass spectrometer was used in conjunction with IR spectroscopy. Initially, the IR-spectrometer was calibrated by recording spectra of isoprene samples with known concentrations contained in a gas-cell with a 4 cm path length. The IR spectra and their corresponding partial pressure of isoprene are shown in Figure 14. Using integration with a sloped baseline, the peak from 2678-3271 cm^{-1} was integrated to produce the integrated absorbance. This peak corresponds to the alkane and alkene functional groups of the isoprene molecule and is proportional to the amount of isoprene present according to Beer's law.
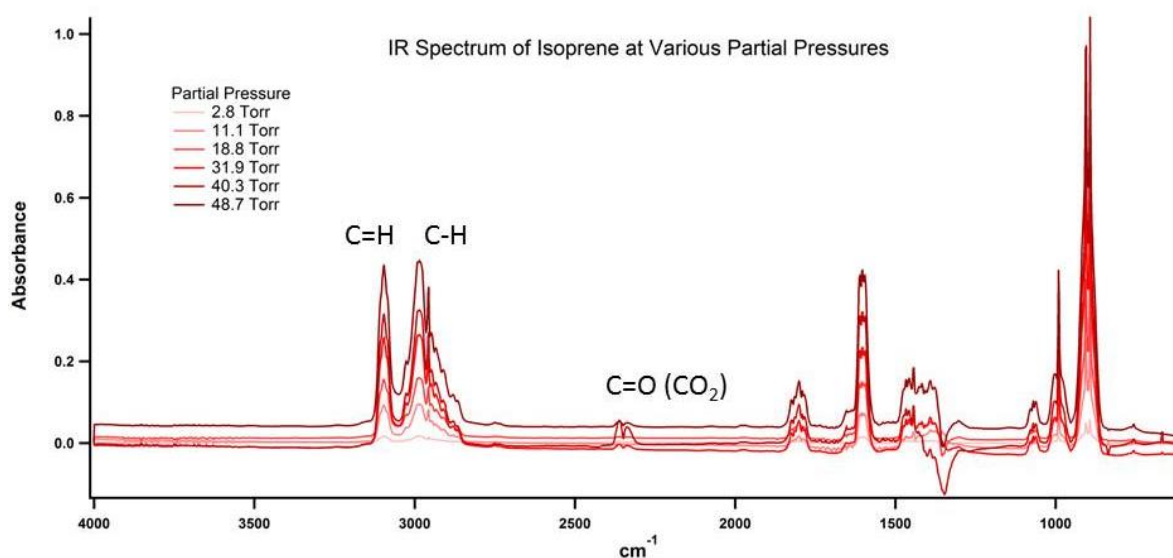
Figure 14. IR spectra of isoprene recorded at different partial pressures using an FTIR gas cell with a path length of 1 cm^{-1}. The absorbance at 2900-3100 cm^{-1} corresponds to isoprene.

The integrated absorbance for each standard was then plotted against the corresponding partial pressure of isoprene within the gas cell. The partial pressure of a gas is proportional to its concentration. This produced a calibration curve which tracks the change of absorbance with respect to a change in concentration. A calibration curve utilizes the Beer's Law equation, $Abs = \sigma Nl$. Where Abs is absorbance, l is the path length of the cell, and σ is the cross section coefficient. Plotting absorbance vs concentration produces a straight line as shown in Figure 15. The equation of the line (y = mx + b) for this graph provides a relationship between absorbance and concentration where the slope is equal to the product of the extinction coefficient and the path length. With a known absorbance value, the equation of the line can be applied to calculate the unknown concentration of a sample. In Figure 15, the value m corresponds to the slope and the value b corresponds to the y-intercept.

IR Spectroscopy Calibration Curve for Isoprene

Coefficient values ± one standard deviation
a $=0.042099 \pm 0.473$
b $=0.57783 \pm 0.0159$
R^2 $=0.9970$
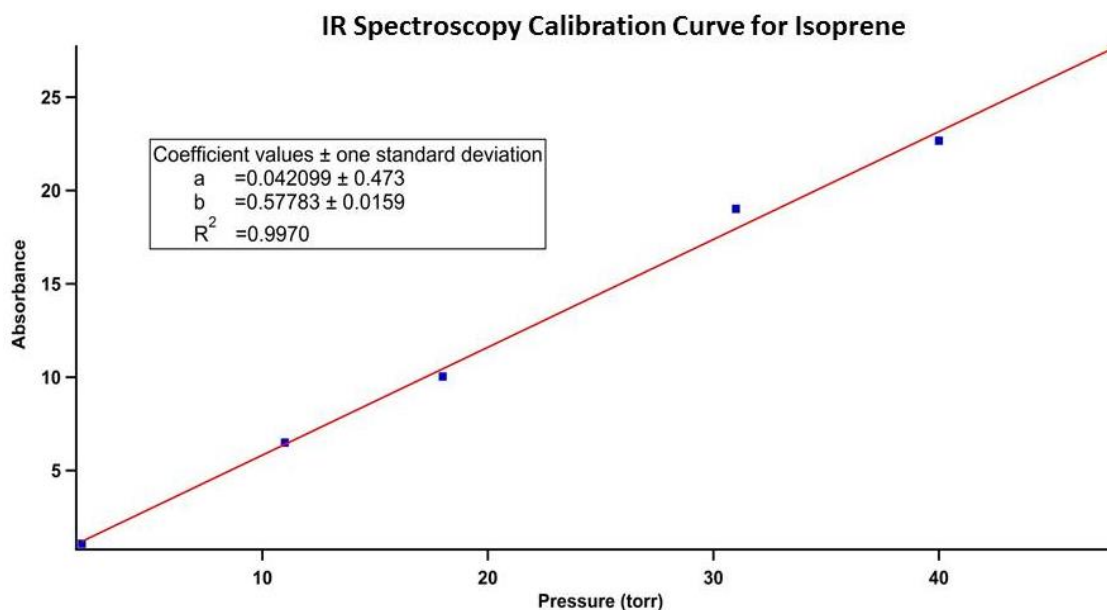
Figure 15: Beer's law was used to produce a calibration curve of absorbance vs partial pressure curve that can be used to find the concentration of a sample with an unknown concentration.

Once the IR spectrometer calibration was complete, the IR spectrometer could be used in further calibrations of the HPR-20 mass spectrometer. To calibrate, the laminar flow reactor was connected to both the IR spectrometer and the mass spectrometer. With the instrument recording, isoprene was introduced into the system at a constant intensity for a set period of time. Five different intensities of isoprene where recorded using the instruments in tandem as shown in Figure 16.
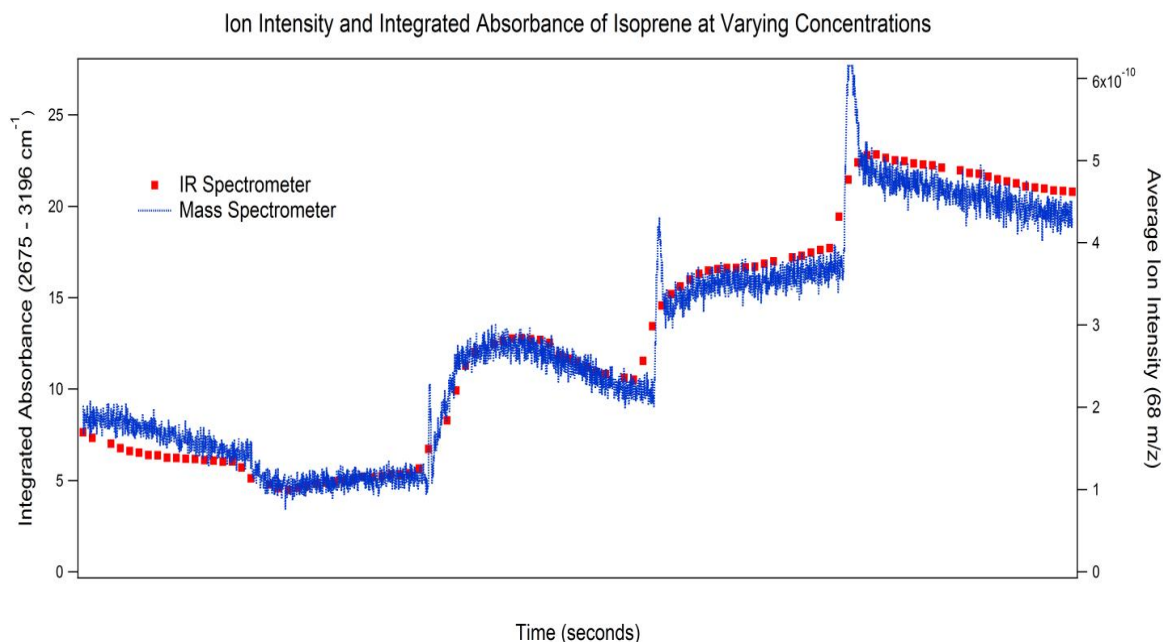
Figure 16: The plot of isoprene intensity from the mass spectrometer and the IR spectrometer. Isoprene concentration was varied 5 times during the course of the experiment.

Using the averaged data from Figure 16, the ion intensity can be compared to the average integrate absorbance to determine the concentration in the flow reactor. The linear relationship between ion intensity and absorbance as shown in Figure 17 facilitated the conversion of ion intensity to concentration in ppm (parts per million). First, partial pressure was converted to concentration by dividing the partial pressure of isoprene (Torr) in the gas cell by total atmospheric pressure (760 Torr) and multiplying the value by a million to give concentration of isoprene in ppm. Due to the linear relationship between ion intensity and integrated absorbance, the known concentration at a specific integrated absorbance defined the concentration at the corresponding ion intensity.
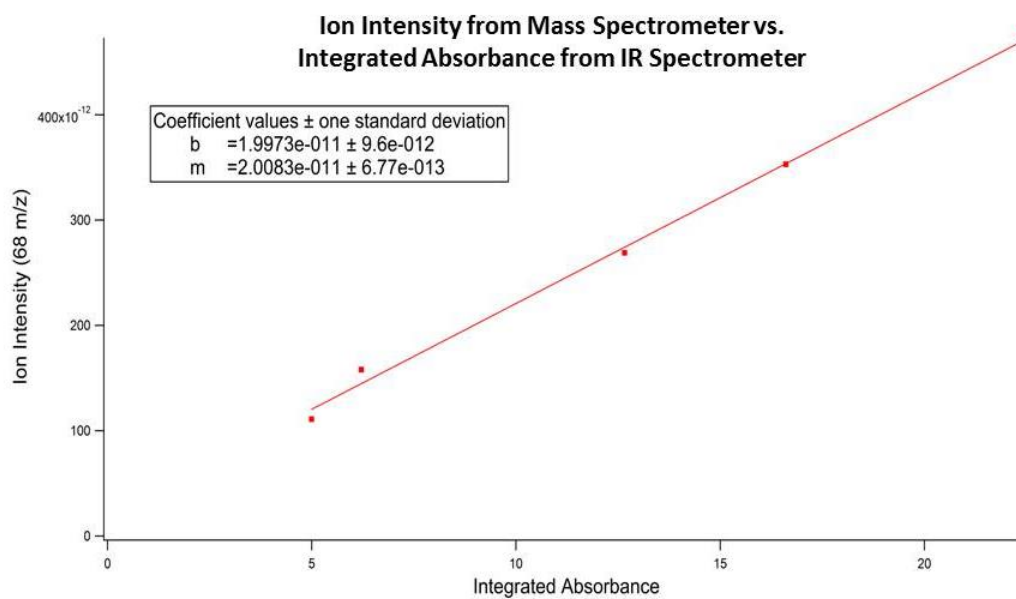
Figure 17: Average ion intensity as recorded by mass spectrometer vs. the integrated absorbance from IR spectroscopy displays a linear relationship.

Lastly, ion intensity was plotted against its corresponding concentration in ppm to produce a calibration curve (Figure 18). This calibration curve has an equation of the line that can be used to calculate an unknown isoprene concentration from a known ion intensity of peak 68 m/z as recorded by the mass spectrometer. The range of the calibration curve is approximately 50 ppm to 240 ppm (Table 5).
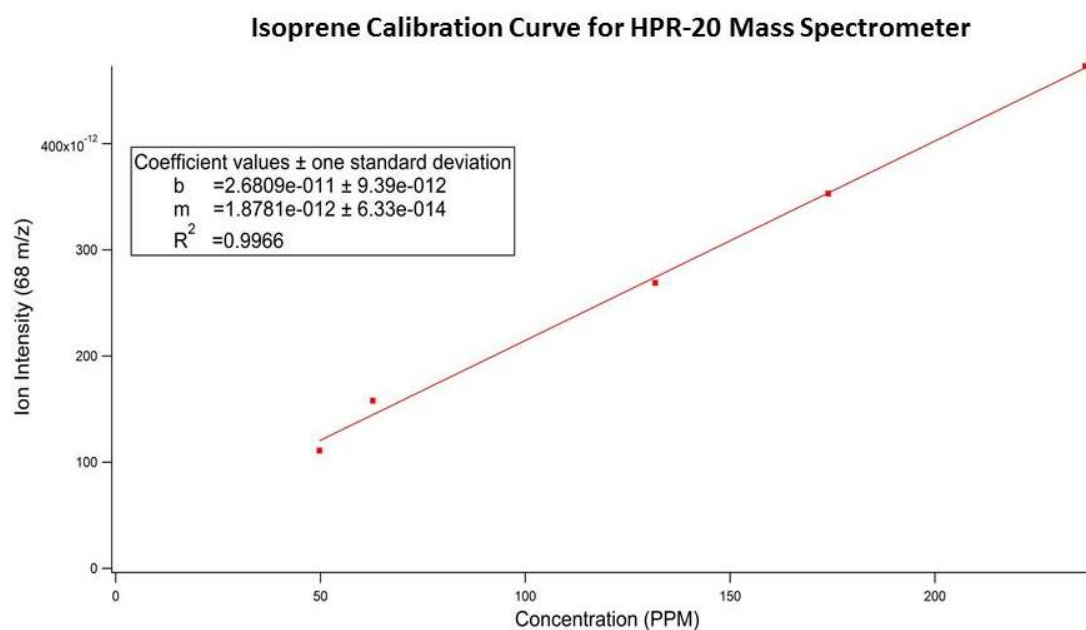
Figure 18: The plot of ion intensity from the mass spectrometer against the concentration in ppm. This curve allows for the calculation of an unknown isoprene concentration that is between 50 ppm to 240 ppm.

PPM	Ion Intensity
50	1.11E-10
63	1.58E-10
130	2.69E-10
170	3.53E-10
240	4.73E-10

Table 5. Concentration and the corresponding ion intensity of isoprene for the calibration of the HPR -20 Mass Spectrometer as shown in Figure 15.

2.5 Calibration of the Laminar Flow Reactor

Several design features and experimental procedures were altered during the construction and calibrating of the flow reactor. During initial construction, the flow reactor was initially assembled with a glass injector rod, however the glass injector rod was too flexible and would bend upon full insertion into the flow reactor while scraping the kaolinite coated sides. To avoid bending, the glass injector rod was replaced by a stainless steel injector rod with the same proportions. The stainless steel shows less bend once fully inserted into the flow reactor and its strength allows it to be manipulated to not scrape the kaolinite coating.

Isoprene has a freezing point of -144 ^{o}C and a boiling point of 34. ^{o}C. At 68 amu, isoprene is a relatively light molecule with high volatility due to its low molecular weight and weak London dispersion forces. Isoprene readily evaporates due to these factors and is easily transported by the nitrogen flow into the flow reactor. Due to the sensitivity of the mass spectrometer, the isoprene in the bubbler must be kept in a cooling bath as to not flood the mass spectrometer with excessive isoprene. Keeping the isoprene below room temperature decreases the vapor pressure, which in turn decreases the rate at which isoprene vaporizes and a lower concentration of isoprene passes through into the flow reactor. Several ice slurry mixtures contained in laboratory Dewar flasks were tested as possible cooling baths to maintain the low temperature. Initially mixed ortho-, para-, and meta- xylene isomers and dry ice was used to create an ice slurry mixture, however this was found to freeze the isoprene. Other cooling baths tested included 1) meta-xylene and dry ice with a temperature of approximately -47°C, which did not have a great effect at

decreasing the isoprene volatility and 2) liquid nitrogen and acetone at approximately -94°C, which proved to be too unstable in maintaining the isoprene concentration at higher flow rates. Dry ice and acetone with literature values of -78°C and a temperature of -70°C in lab was ultimately chosen for its stability and temperature range. To further enhance the stability of the cooling bath temperature and therefore the isoprene concentration, the acetone and dry ice mixture must be thoroughly mixed in five minute intervals throughout the course of an experiment.

Flow rates were optimized by running control experiments without the presence of kaolinite, where uncoated tubes are referred to as "blank" reactions. At lower flow rates, the moving of the injector rod introduces a drop in ion intensity. Pulling the injector rod out of the flow reactor introduces a brief dip in ion intensity and pushing the injector rod back into the flow reactor introduces a spike that is similar in intensity and time as shown in Figure 16. The drop in ion intensity also occurs during a decrease in isoprene concentration due to reaction and therefore this drop in ion intensity needs to be minimized for an accurate experiment. The blank reactions are used to account for any error introduced by the moving of the injector rod. This error can be minimized by increasing the flow rate by several thousand SCCM, which reduces the intensity and duration of the drop in ion intensity that creates the error. Figure 19 compares two reaction simulations at similar ion intensities of approximately 2.4x10^{-10} (100 ppm) using two different flow rates at 1200 SCCM and 8,500 SCCM.
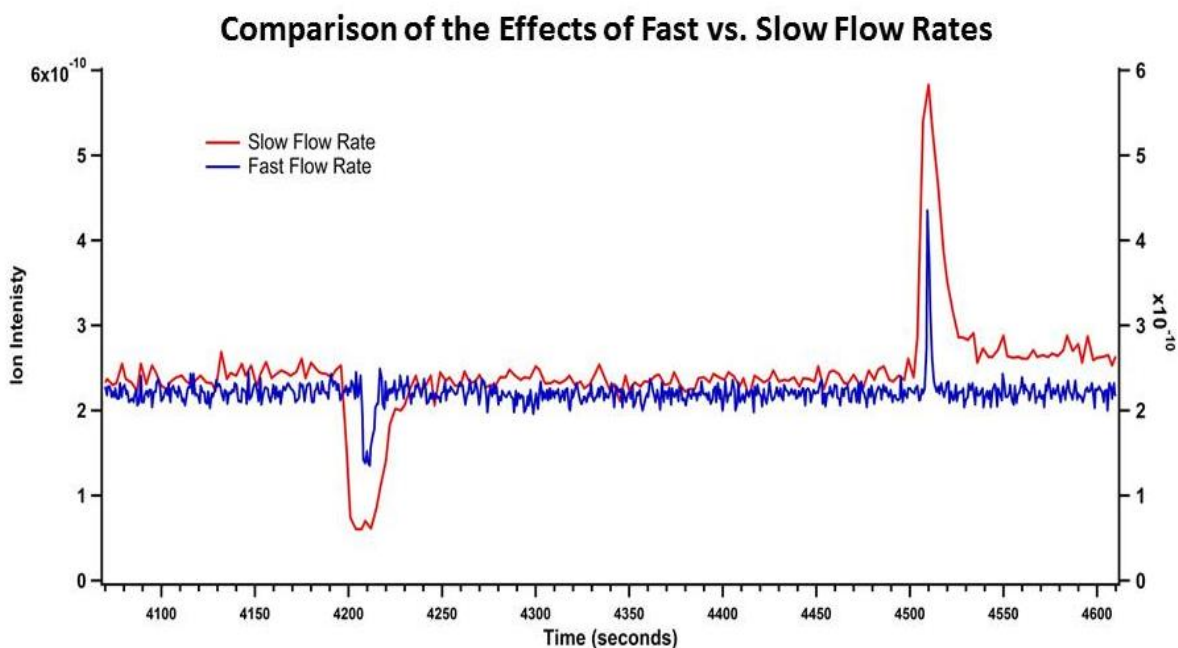
Figure 19: A comparison of the error produced from moving the injector rod in the flow reactor at slow rates vs. fast flow rates. This error is reduced at high flow rates.

Increasing the flow rate to 8500 SCCM reduced the duration of the drop in ion intensity from approximately 40 seconds to approximately 20 seconds, which decreases the drop in ion intensity time by half. The height of the dip was reduced from 6.1×10^{-11} to 1.4×10^{-10}, thus reducing the dip by 130 percent and the height of the spike was reduced from 5.8×10^{-10} to 4.4×10^{-10}, reducing the spike by 24 percent. Reducing the drop in ion intensity allows for more accurate kinetic and uptake coefficient measurements at early reaction times. It is possible the drop in ion intensity could be further reduced by further increasing the flow rate, however the system was not designed for such high flow rates and another further increase would be hazardous. Decreasing the concentration of isoprene also decreases the size of the drop in ion intensities produced; however the noise

level of the mass spectrometer becomes too large at concentrations lower than 50 ppm due to the detection abilities of the instrument. Therefore the data for the reaction between 100 ppm isoprene and kaolinite in the laminar flow reactor is optimized at approximately 8,500 SCCM.

The reactivity of isoprene decreases as water is introduced into the system due to competitive adsorption due to water saturating the active sites so that isoprene cannot react with the kaolinite surface. Therefore reactivity is optimized in the absence of water. Initially, kaolinite slurries were prepared with semi-volatile organic solvents that were quick to dry such as chloroform. However these compounds were found to dry too fast and produced a thick uneven layer of kaolinite coating. Sulfuric acid was also tested as a possible liquid, however upon the addition and drying of sulfuric acid, isoprene showed less reactivity towards kaolinite. It was determined that deionized water and kaolinite in a 2:1 ratio produced the best slurry quality in terms of consistency and produced a thin and even layer of kaolinite coating. However, the water and kaolinite slurry required the longest drying time of lengths greater than 24 hours to ensure complete evaporation of the water. This process could be accompanied by flowing nitrogen gas to enhance drying and shorten the time required to completely dry the coating. Multiple coating techniques were also tested. Pouring the kaolinite slurry into the tube held at an angle produced an even coating that could be manipulated into coating only portions of the tube. The pouring method is best for partial coatings however this method does produced a thick coating with several layers. A wire-bristle brush with an extended handle provides complete coverage with a thin and even coating. To achieve coating with the brush, half

of the kaolinite slurry is initially poured into the tube followed by the brush being rotated to spread the mixture to half the tube and this technique is repeated on the opposing side to ensure coverage of the entire length of the tube.

Initial experiments used kaolin (Sigma Aldrich), which is a finely processed powder, while later experiments used High Defect Kaolinite from the Clay Mineral Society. The high defect kaolinite showed greater reactivity with isoprene when compared to the kaolin as shown in Figure 20. When isoprene is introduced to the high defect kaolinite, there is a greater decrease in isoprene concentration compared to the kaolin surface which indicates that more isoprene molecules are adsorbing onto the high defect kaolinite surface. The recovery difference is due to the difference in flow rates and therefore a difference in number of gaseous isoprene collisions with kaolinite. Both kaolin and high defect kaolinite will make a full recovery given enough time.
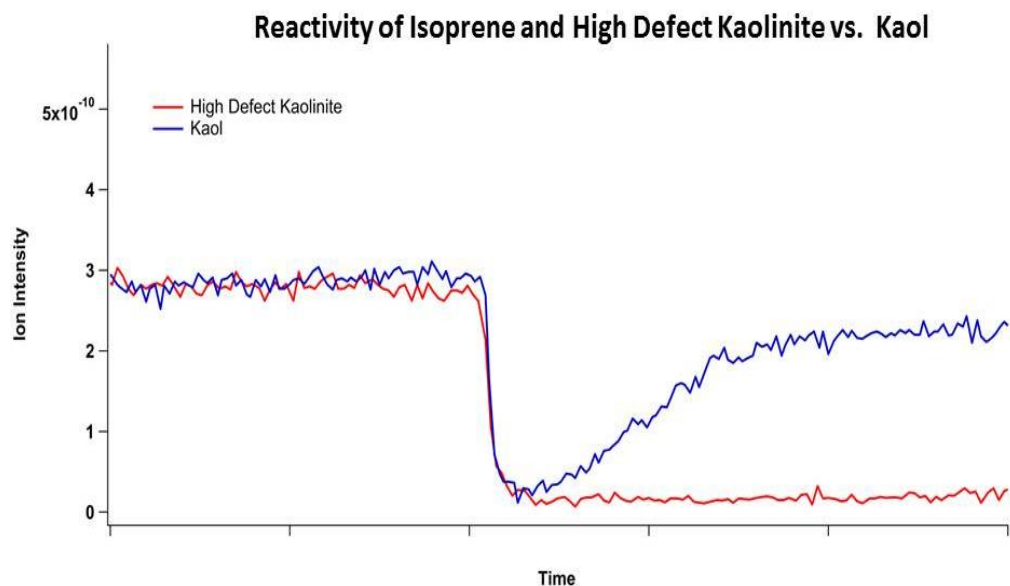
Figure 20: The comparison of isoprene reactivity in the presence of high defect kaolinite vs. kaolin (processed).

2.6 Experimental Methods

The laminar flow reactor as described above undergoes the following preparation to monitor the heterogeneous reaction of isoprene and kaolinite. A kaolinite slurry is prepared using approximately 12 grams of kaolinite and 25 mL of deionized water. Using a bristled brush, the 122-cm long glass tube with an inner diameter of 2.5-cm is coated with a thin layer of kaolinite slurry. The tube is then inserted into the flow reactor with flowing nitrogen gas at 60 SCCM and is allowed to dry over a 24 hour period, with occasional rotations to ensure an even coating. Once dried, the flow reactor is re-assembled for the experiment. At this time, the movable injector rod is fully inserted to avoid kaolinite and isoprene interaction. The isoprene located in the bubbler is

maintained in an environment of approximately -70°C using an acetone and dry ice cooling bath. The isoprene concentration is monitored using the mass spectrometer. Throughout the course of the experiment, the molecular ion peak (68 m/z) is observed to monitor changes in isoprene concentration.

The positioning of the injector rod throughout the course of the experiment is displayed in Figure 21. Initially, the injector rod is fully inserted into the flow reactor as shown in Figure 21 (a). Due to the constant stream of nitrogen gas and the forward moving flow of isoprene, there is no interaction between the isoprene being emitted from the injector rod and the kaolinite coating that lies behind the injector rod outlet. At this point the isoprene concentration is allowed to stabilize. Once stabilization occurs, the injector rod is pulled back to a set distance to expose the kaolinite coating to isoprene as shown in Figure 21 (b).
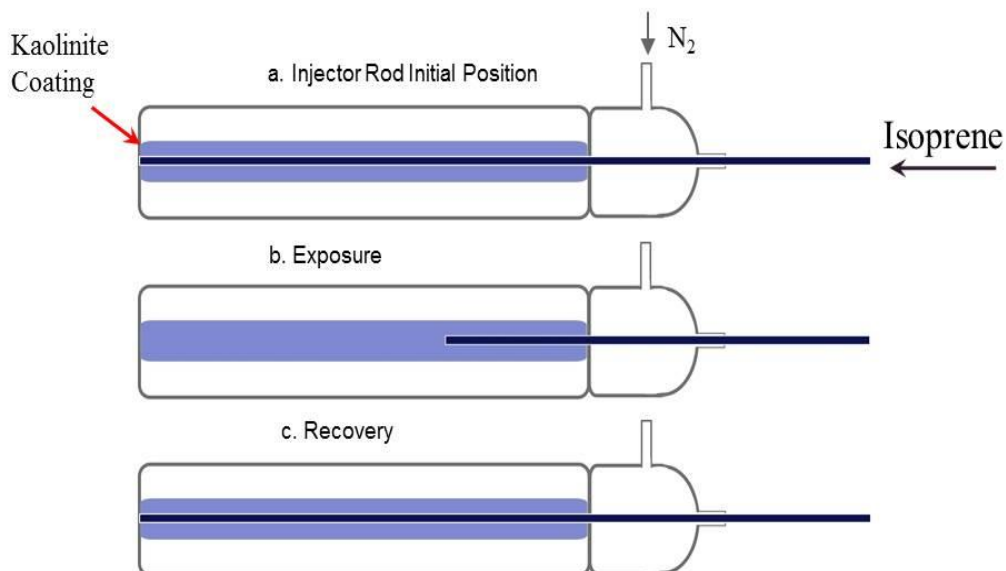
Figure 21: Positions of the injector rod throughout the course of the experiment. Initially, the injector rod is fully inserted into the flow reactor (a.). The injector rod is then pulled back to expose the kaolinite to isoprene (position b.), and is returned to its initial position during recovery (c.).

Pulling the injector rod back by some degree allows isoprene to interact with the kaolinite coating, and the changes in isoprene concentration due to adsorption and reactivity is recorded by the mass spectrometer as a decrease in ion intensity as shown in Figure 22. Once the concentration begins to reach a new equilibrium point, the injector rod is returned to the fully inserted position as shown in Figure 21 (c) to stop the interaction between isoprene and kaolinite. At this point, isoprene levels return to initial concentration as shown in Figure 22. The amount of isoprene being injected into the flow reactor and rate at which it enters remains constant throughout the course of the experiment. Due to the mass spectrometer recording the concentration of exiting molecules at the end of the flow reactor, any changes in concentration that occur during

exposure can be attributed to loss of isoprene from adsorption and reactivity between the gas and surface coating.
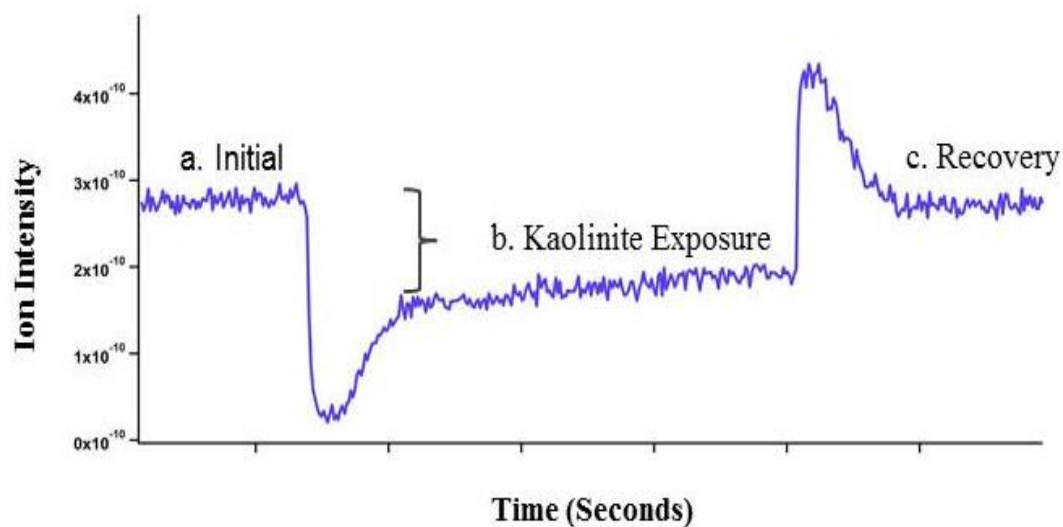
Figure 22: The reaction progress as recorded by the gas-analysis mass spectrometer. Part a. corresponds to the initial stabilized isoprene concentration, b. corresponds to the kaolinite coating being exposed to isoprene, and c. is the recovery period. The decrease in part b. indicates isoprene reactivity with the kaolinite.

2.7 Calculations

Heterogeneous reactions, such as the one under study, are often defined by the corresponding reactive uptake coefficient because it can be used to evaluate the significance of the reaction in the atmosphere (Liggio et al., 2006). The reactive uptake coefficient, referred to as γ, is the number of collisions with the surface that leads to a reaction. Reactive uptake coefficients can be experimentally calculated by monitoring the loss of gaseous species due to reactions with the surface material. Previously, the uptake coefficient was calculated using the DRIFTS method and reacting isoprene with a

kaolinite sample in a DRIFTS chamber. Our new method includes the use of the laminar flow reactor to calculate uptake coefficients. The shortened residence time in the flow reactor gives improved kinetics calculations and therefore improved uptake coefficients over the extended residence time of the gas cell and DRIFTS method that was previously used. This allows for an almost instantaneous measurement of the reaction uptake.
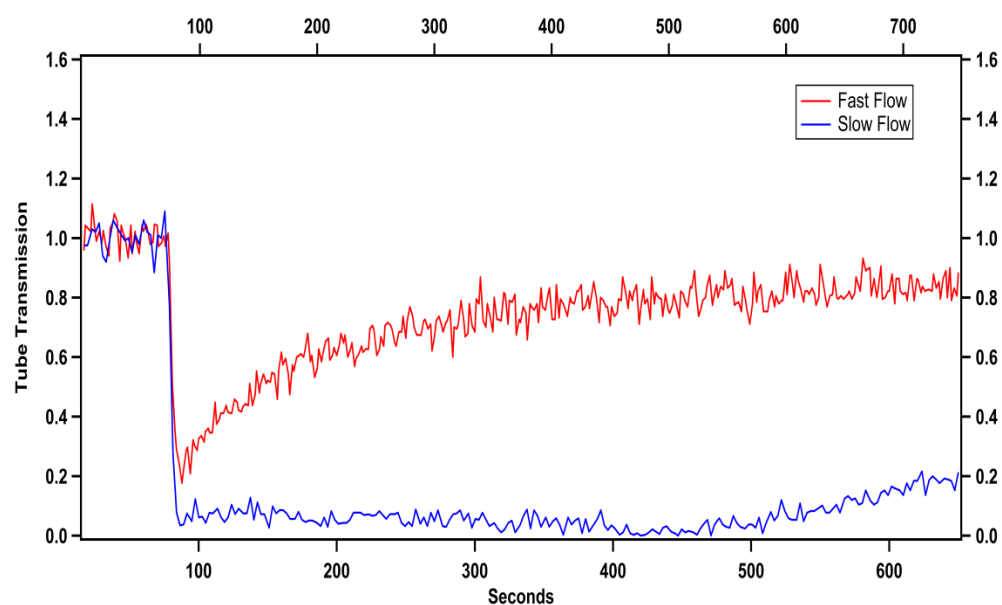
Figure 23. The measured tube transmission for the uptake of isoprene on kaolinite in the laminar flow reactor for both fast and slow flow rates.

As established, the laminar flow reactor monitors the changes in isoprene concentration due to reactive uptake of isoprene molecules on the kaolinite surface. By monitoring the concentration changes, the tube transmission is measured which is the number of molecules escaping the flow reactor to the mass spectrometer relative to the average initial concentration of isoprene (Tube transmission = $[iso]/[iso]_o$). Figure 23 compares the tube transmission for fast flow rates (8500 SCCCM) with the tube

transmission for slow flow rates (1200 SCCM) plotted versus time of reaction. Both flow rates provide the same final tube transmission, however the faster flow rate results in better initial uptake calculations due to the optimization as previously discussed. The experimentally observed tube transmission can be used to determine the net (or effective) uptake coefficient (γ_{eff}) following Equation 5.

Equation 5.
$$\gamma_{eff,isoprene} = \frac{D_{tube}}{\omega_x t} * ln\left(\frac{[isoprene]_0}{[isoprene]_s}\right)$$

The effective uptake coefficient can be used to calculate the uptake coefficient (γ) that includes the addition of necessary adjustments as outlined above to correct for diffusion effects (Equation 6) (Knopf et al. 2015).

Equation 6.
$$\gamma = \frac{\gamma_{eff,isoprene}}{1-\gamma_{eff,isoprene}*\frac{3}{2N_{Shw}^{eff}Kn}}$$

Due to the initial drop in ion intensity in the data, the first 20 seconds of data points were ignored. At fast flow rates, the initial uptake coefficient for isoprene on the kaolinite surface is 1.3×10^{-4} for dry conditions. The effective uptake coefficient and the uptake coefficient without adjustments as a function of reaction time can be seen in Figure 24. The effective uptake coefficient corrects for flow parameters, and thus is a more accurate value and it should be noted that the effective uptake coefficient is larger than the unadjusted uptake coefficient at initial data points. Therefore, other calculation methods would under predict the initial uptake coefficient, and give imprecise values that are not true representation of the reaction.
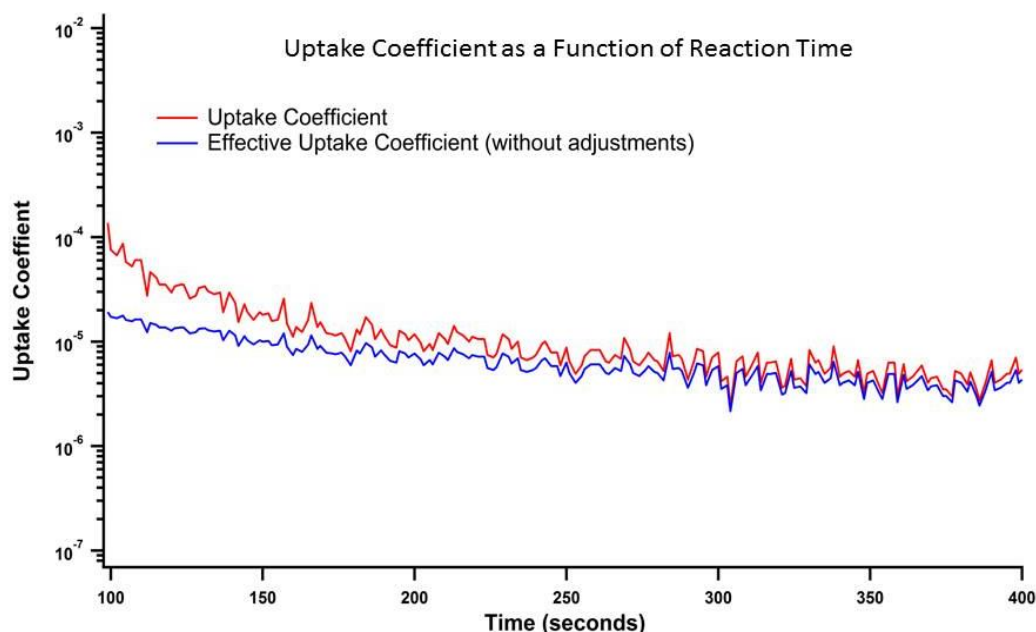
Figure 24. The uptake coefficient on log scale as a function of time for the heterogeneous reaction of isoprene and kaolinite for both the effective uptake coefficient and the uptake coefficient without adjustments. The actual uptake coefficient accounts for gas diffusion effects and provides better kinetic calculations especially at initial data points.

Given enough time, the tube transmission will return to a value of 1 thus indicating that kaolinite reaches a point of saturation and isoprene ceases to adsorb onto the surface. Meanwhile, stopping the reaction early by pushing the injector rod back into the initial position produces an excess of isoprene as indicated by the increase in ion intensity that decays back to the initial concentration as shown by Figure 19. This indicates some reversible adsorption of the isoprene molecules. However, not all of the isoprene molecules are regained thereby indicating irreversible adsorption due to reactions with the kaolinite surface itself. It was calculated that approximately 6.5×10^{20} molecules/m^2 are irreversibly adsorbing out of 3.3×10^{21} molecules/m^2 expected. In other terms, 1 in every 10,000 collisions results in reactive uptake.

Chapter 3- Product Identification

3.1 Drifts Analysis
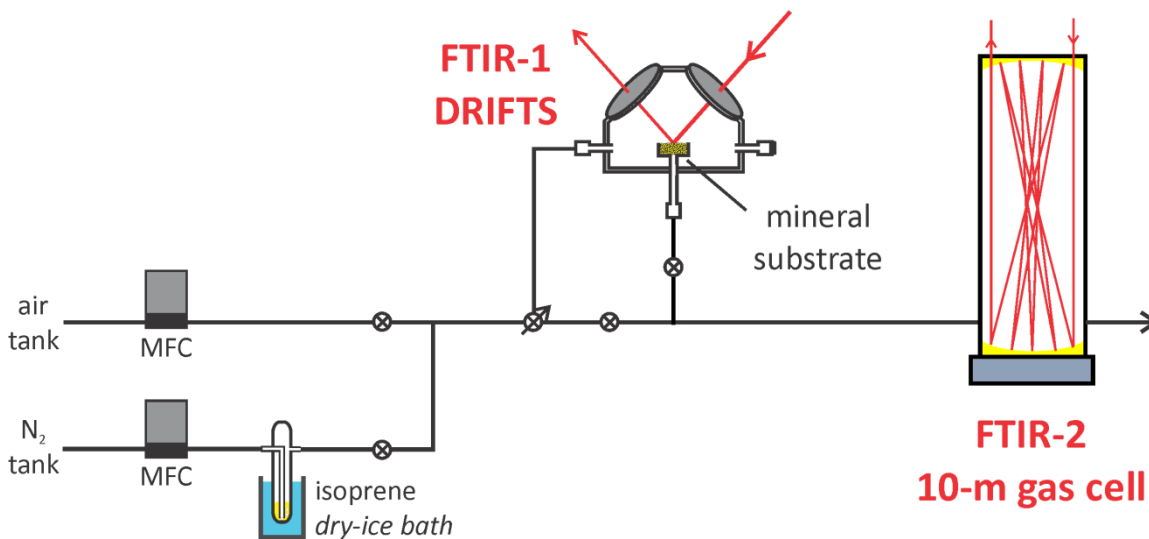
Figure 25. Setup for Diffuse Reflectance Infrared Fourier Transform Spectroscopy (DRIFTS). Kaolinite is packed into a DRIFTS chamber and gaseous isoprene is flowed over the kaolinite. An FTIR instrument detects surface level concentrations throughout the experiment.

Diffuse Reflectance Infrared Fourier Transform Spectroscopy (DRIFTS) was used to further monitor the heterogeneous reaction between isoprene and kaolinite. Mineral powders have particles randomly orientated in space that results in reflection of light in all directions, which is referred to as diffuse reflection, that can be collected by a DRIFTS accessory (Figure 25) (Ulery et al., 2008). The DRIFTS chamber is connected to a Nicolet 6700 Fourier Transform Infrared (FTIR) spectrometer that records IR spectra that monitors changes in the mineral sample. Kaolinite with a calcium carbonate bottom layer is packed into a sample cup in the DRIFTS chamber, and the sample is purged for 24 hours with continuous nitrogen gas flow to remove any surface water. Isoprene in a bubbler submerged in a dry ice and acetone ice bath is introduced into the chamber along

with the carrier gas for a net flow of 300 SCCM. IR spectra are continuously collected for

the reaction over a 20 hour period. The DRIFTS chamber is isolated at the completion

point. The growth of organic compounds on the kaolinite sample is evident in the

produced IR spectra (Figure 26). Formation of the peak ranging from 2800-3000 cm^{-1}

indicates carbon-hydrogen bonds belonging to an organic compound, the peak increases

in magnitude as time elapses as the kaolinite begins to reach a saturation point. There is

also a peak formed at the 3100 cm^{-1} belonging to an alkene that appears in the midpoint

of the data set. This peak disappears shortly after its appearance indicating that a

sequential reaction may be occurring.
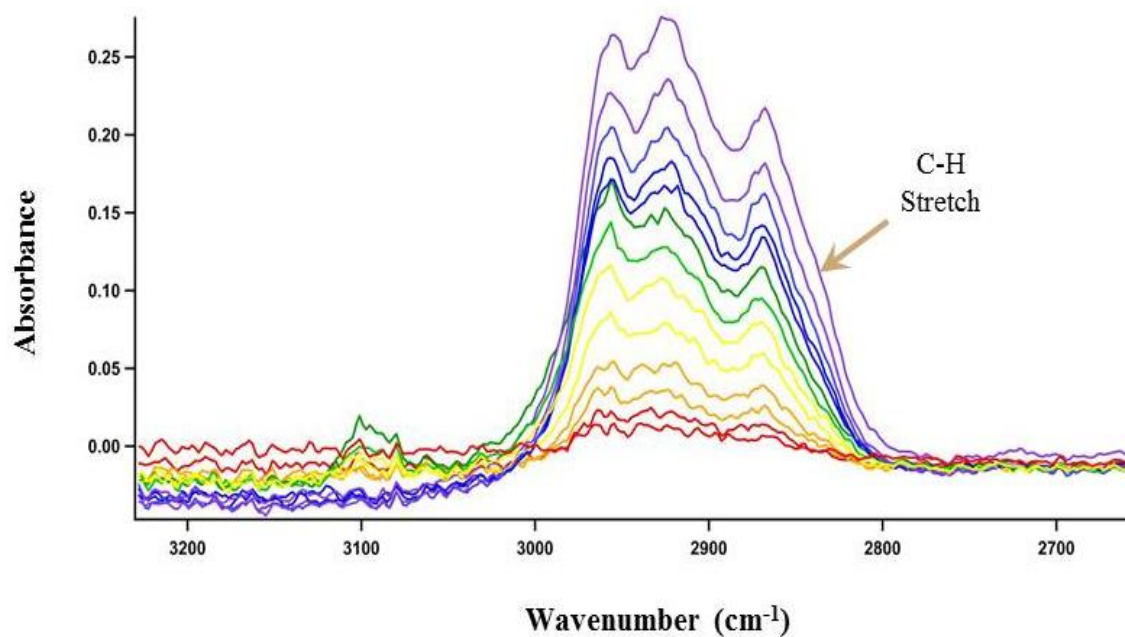
Figure 26. The IR spectra from the DRIFTS monitored reaction between isoprene and kaolinite. The peak
at 2800-3000 indicates organic product formation on the kaolinite surface. The appearance of an alkene
peak at 3100 cm^{-1} indicates a sequential reaction or a surge in isoprene concentration.

Integration with a sloped baseline was performed for both the alkane and alkene peaks and plotted as a function of time in Figure 27. The integrated absorbance shows the growth (and disappearance) of the peak over the course of the reaction. An increase in alkane and alkene integrated absorbance occurs simultaneously, this indicates that a surge in isoprene concentration occurred during at approximately 250 seconds this shifting the equilibrium of the reversibly adsorbed isoprene. However, further testing is needed to determine if alkene peak is a result of a sequential reaction or surge in isoprene concentration.

Figure 27. The integration absorbance as a function of reaction time for the alkane peak (red) and the alkene peak (blue). The rapid increase for both the alkane and alkene at approximately 250 seconds indicates a possible surge in isoprene concentration which shifted the equilibria of reversibly adsorbed isoprene.

3.2 GC-MS Analysis

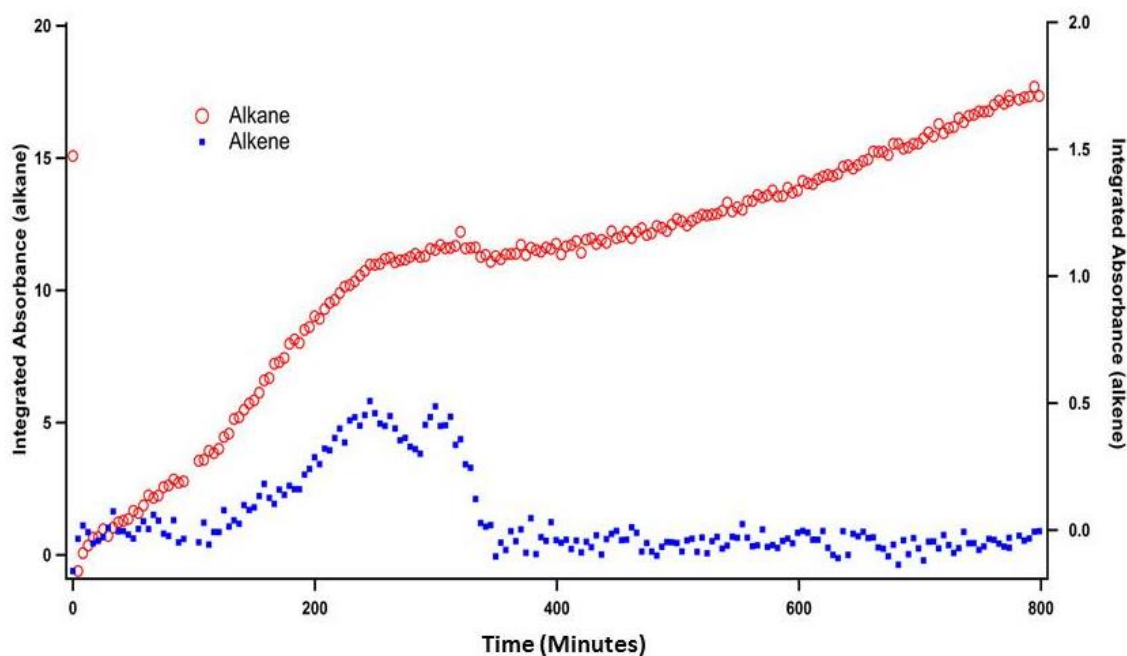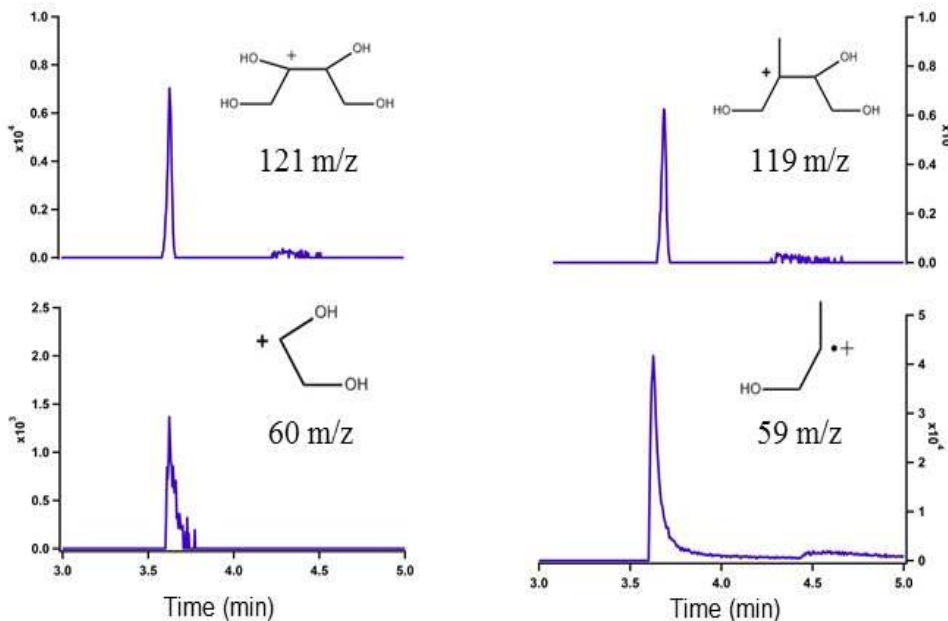**Figure 28.** The extracted ion chromatograms of the organic product from the DRIFTS reaction. The retention time of the product is identified at 3.53 minutes. Ion fragments of 121, 119, 60, and 50 m/z corresponds to the product. A molecular ion peak of 136 m/z was not found, however the suggested fragmentation pattern for 2-methyl tetrol matches the observed ions.

The adsorbed organic compounds from the DRIFTS samples were extracted for further analysis by GC-MS. The top layer of the kaolinite sample was sonicated in 1 mL acetonitrile for 25 minutes and filtered using 0.25 μm syringe filter (Whatman) into GC-MS amber glass vials. Following extraction, samples were analyzed by GC-MS for a total run time of 27 minutes. Initial oven temperature were set at 50°C for a five minute hold time and a solvent delay of 2 minutes, followed by a 10 °C increase in temperature per minute with a maximum temperature of 250 °C and the maximum oven temperature was held for 2 minutes. Extracted ion chromatograms were used to identify the organic compounds and their retention times. The retention time of the main product was

determined to be 3.53 minutes and four ions were identified as belonging to the product

as shown in Figure 28. The ions matched to the product were 121 m/z, 119 m/z, 60 m/z,

and 59 m/z and the respective ion fragment is included with each extracted ion

chromatogram in Figure 28. No parent ion is observed. Fragmentation pattern is

consistent with the 2-methyl tetrol (Scheme 5).
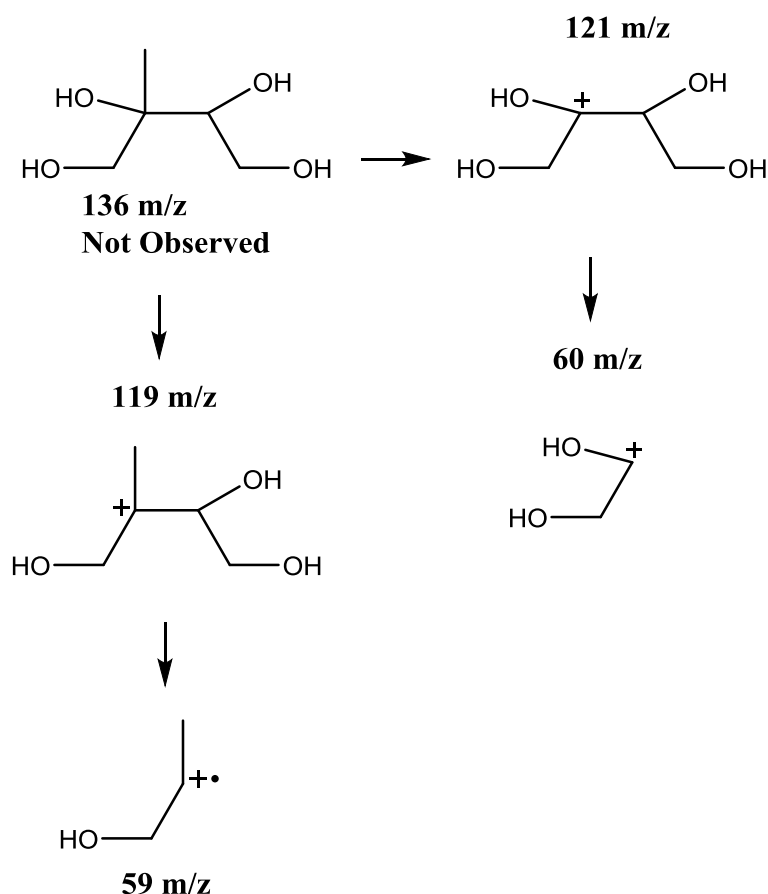
Scheme 5. Suggested fragmentation pattern for 2-methyl tetrol, the suggested product for the
heterogeneous reaction of isoprene and kaolinite.

Commercial 2-C-methyl-erythritol, a 2-methyl tetrol isomer, was purchased to use

as a standard. The 1 mg sample was diluted with the addition of 20 mL deuterated

acetonitrile to make a 200 ppm stock solution. Additional diluted samples were made from stock solution directly in the GC-MS vials for testing. The standard samples were directly analyzed using the GC-MS methods previously outlined for the unknown sample. Extracted ion chromatograms were used to identify the 2-C-methyl-erythritol retention time at 3.54 minutes. Ion fragments that corresponded to the 2-C-methyl-erythritol were 123 m/z, 121 m/z, 64 m/z, 63 m/z, and 46 m/z. These ion fragments were unexpected for the 2-C-methyl-erythritol, with values approximately 2 units higher than predicted. Even though it seems unlikely, we propose possible partial deuteration from the deuterated acetonitrile solvent as an explanation for the abnormal peaks such as 123 m/z. The ion fragments suggest that the 2-C-methyl-erythritol was partially deuterated and produced the fragmentation pattern as suggested in Scheme 6. However, it still remains unknown to us as to why the ion fragments were only 2 units higher than expected values and more

testing needs to be completed for a better analysis that is outside the scope of this project.
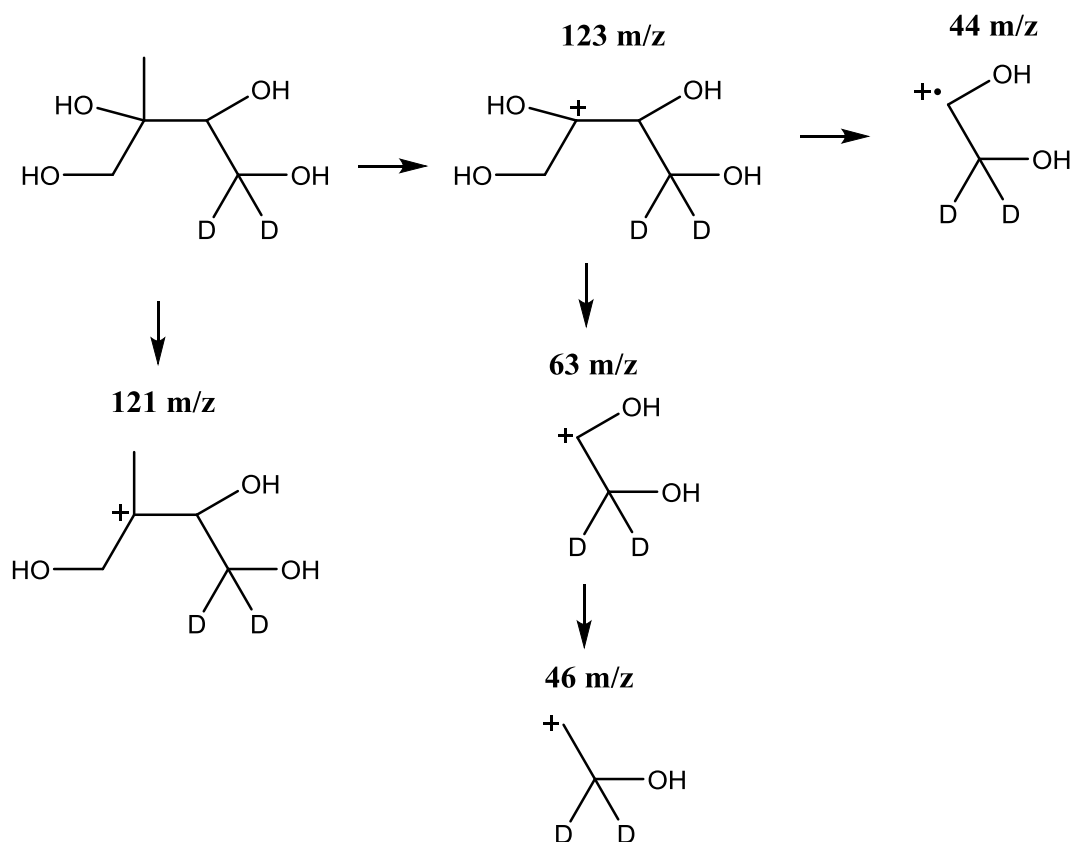
Scheme 6. The suggested fragmentation pattern of the partially deuterated 2-methyl tetrol in deuterated acetonitrile. Further testing is needed to explain the differences in ion fragments between the product in acetonitrile and deuterated-acetonitrile.

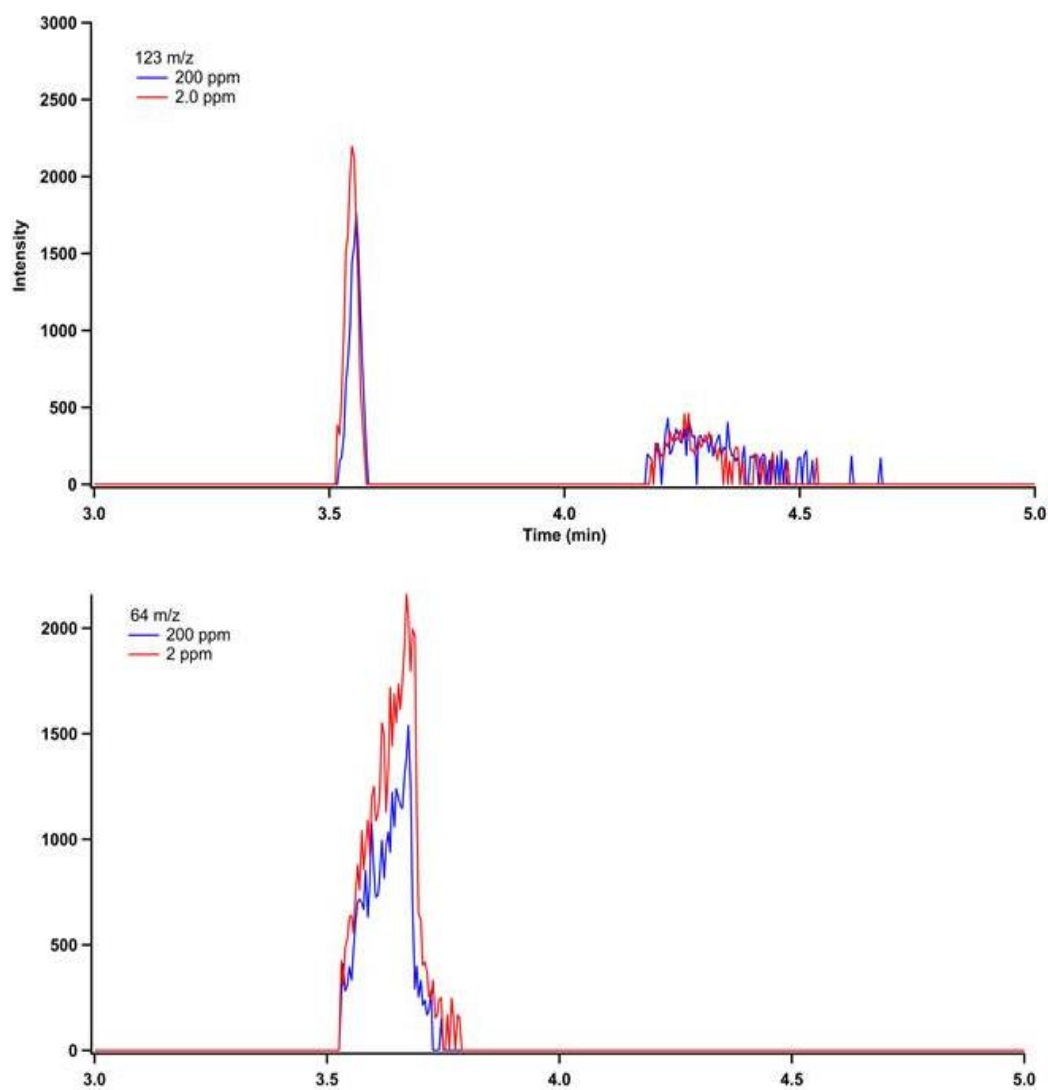## 3.3 Stability of 2-C-methyl-erythritol

Figure 29. The extracted ion chromatograms for the 2-C-methyl-erythritol standard. The red line indicates the 2.0 ppm sample while the blue line is the 200 ppm sample tested approximately 110 minutes later. The decrease in concentration due to time and not to concentration indicates 2-C-methyl-erythritol decays over a short period of time and is not stable.

Originally, the samples were analyzed to create a calibration curve. However GC-MS analysis showed that 2-C-methyl-erythritol in the samples decayed over a short period of time rendering this method insufficient. As the 2-C-methyl-erythritol decayed, the retention time increased and shifted to the right of the extracted ion chromatogram as shown in Figure 29. Initially, a 2.0 ppm sample of the 2-C-methyl-erythritol was analyzed using the above GC-MS method given by the red line in Figure 29. Approximately 110 minutes later, a 200 ppm sample of 2-C-methyl-erythritol was analyzed and produced the result as depicted by the blue line in Figure 29, even though the concentration of this sample was 100 fold more than the 2.0 ppm sample, the intensity of the peak significantly decreased in comparison. Figure 29 displays both the 123 m/z and the 64 m/z ions to illustrate the decay. This indicates that 2-C-methyl-erythritol decayed rapidly over the 110 minute time frame. Testing of the sample done at a later time shows the complete disappearance of the 2-C-methyl-eryhtritol indicating that it is unstable in the deuterated acetonitrile, and it can be concluded that 2-C-methyl-eryhtritol is not stable at room temperature. The organic product of the isoprene and kaolinite reaction also decayed over a period of time. The decay of 2-C-methyl-erythritol has implications on its atmospheric lifetime and relevancy as an isoprene-derived product. Further testing is required to determine the decay process and the stability of 2-C-methyl-eryhtritol and all 2-methyl tetrol isomers.

3.4 Comparison of the Adsorbed Organics and 2-C-methyl-eryhtritol

The proposed products for the isoprene and kaolinite reaction are isomers of the 2-methyl tetrol. Further testing of the adsorbed organic compound was performed using deuterated acetonitrile as the solvent to compare it to the 2-C-methyl-erythritol sample in deuterated acetonitrile. The use of deuterated acetonitrile altered extracted ion fragments for the extracted organic compound as well as shift the retention time from 3.53 minutes to 3.50 minutes. The ion chromatograms show the appearance of another bump at approximately 3.54 minute that closely matches the 2-methyl standard. The two bumps indicate multiple products formed during the course of the reaction that may be isomers of each other. The reaction sample extracted in deuterated acetonitrile produces ion fragments of 64 m/z, 63 m/z, and 46 m/z that closely resemble the standard as shown in Figure 30. The slight shift in retention time may be due to instrument maintenance that occurred over the course of the experiment. It is still unknown as to why the deuterated acetonitrile produced changes in the behavior of the organic compound in the GC-MS, and further investigation into the interactions between solvents and organic products need to be performed. However, the close proximity in retention time and the overall shape of the peak suggests that a product of the isoprene and kaolinite reaction is 2-C-methyl-erythritol, an isomer of the 2-methyl tetrol.
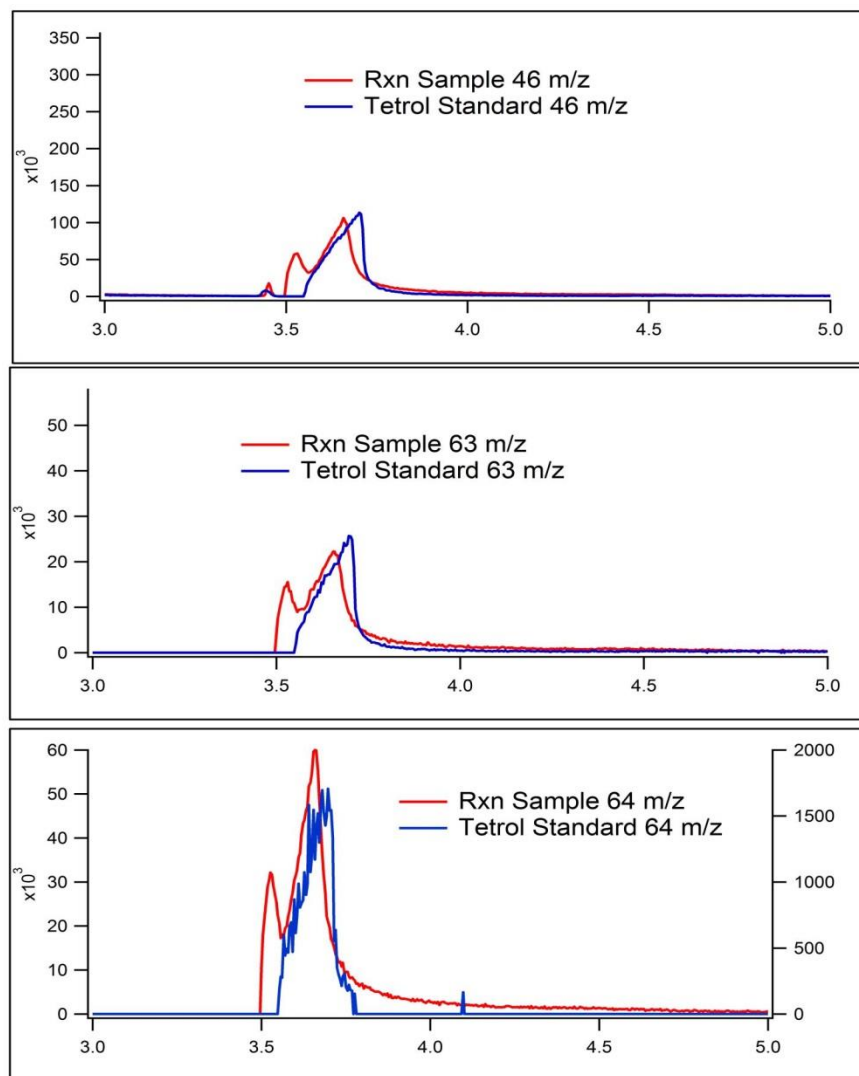
Figure 30. Comparison of extracted ion chromatograms for the 2-methol tetrol standard and the unknown organic compound sample both with deuterated acetonitrile as the solvent provide similar ion fragments.

As previously shown, 2-C-methyl-eryhtritol in deuterated acetonitrile is not stable and can be see rapidly decaying over a short time span. This calls into question the stability of the condensed product formed during the isoprene and kaolinite reaction. In acetonitrile, the organic product also disappeared over a length of time however it appears to be stable while adsorbed onto the kaolinite surface. The DRIFTS method used

to monitor the growth of organic compounds on the kaolinite surface was also used to examine the surface 7 days after the reaction. The organic compounds as seen in the peaks from 3000-2800 cm^{-1} in the IR spectra (Figure 31) still appeared relatively unchanged one week after the reaction. Comparisons were made with a mid-reaction IR spectrum and the kaolinite was maintained the closed DRIFTS chamber. Even though the product is unstable in acetonitrile, it appears to be stable while adsorbed on the kaolinite surface.

Figure 31. The IR spectra for the adsorbed organic compound on kaolinite during the reaction and 1 week after the reaction of isoprene and kaolinite. The similar appearance indicates that the organic product is stable on the surface of the kaolinite.
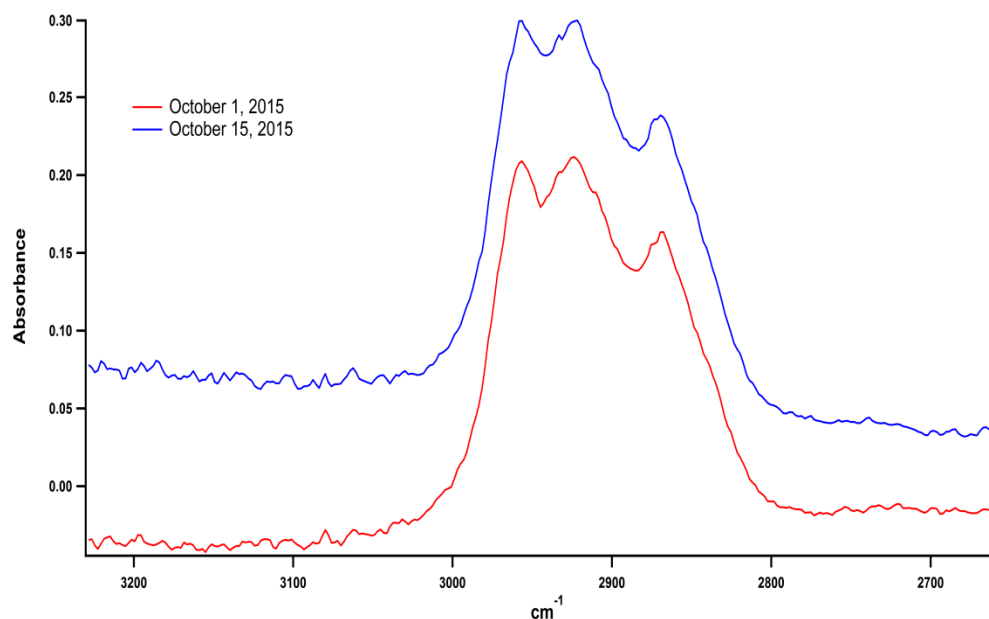
Chapter 4- Discussion and Conclusion

4.1 The Heterogeneous Reaction of Isoprene and Kaolinite

The DRIFTS experiment has confirmed the growth of organic compounds on kaolinite surfaces when exposed to isoprene. Once adsorbed onto the surface, the products are stable for up to a week on undisturbed kaolinite but decay once extracted in acetonitrile as shown by the GC-MS experiment. This calls into question the stability of the organic compound and its impact on atmospheric chemistry. A stable product is more likely to alter the chemical properties of the mineral dust, altering its ice nucleation abilities and radiative forcing. Overall this can affect both cloud formation and the Earth's radiation budget which has greater implications on the climate as a whole. However more testing is needed to determine its stability on the mineral surface as well as in other solvents. Continuation should also include identification of the decay product, which can also contribute changes in aerosol properties.

Testing of the organic compound has provided data in support of our hypothesis that the isoprene and kaolinite reaction produces 2-methyl tetrols. Previously, 2-methyl tetrols have been found in aerosol samples and are suggested to be a significant source of SOA (Ying et al., 2015). These findings suggest that the 2-methyl tetrol is stable in atmospheric conditions which are contrary to our findings. However, our research did suggest that the organic product, which is hypothesized to be the 2-methyl tetrol, is stable on a kaolinite surface. Therefore, it may be possible that the 2-methyl tetrol is only stable when adsorbed to a surface instead of free in solution.

The comparison of the organic product with 2-C-methyl-erythritol suggested that 2-C-methyl-erythritol isomer is produced by the isoprene and kaolinite reaction. We propose that the still unidentified product may be 2-methylthreitol, which is the other 2-methyl tetrol isomer. These findings suggest that 2-methyl tetrols found in aerosols sample may form from isoprene reactions and indicate that isoprene may have a more significant contribution to SOA. However, the significance of this contribution relies on the prominence of isoprene heterogeneous reactions which can be assessed based on uptake coefficients. The condensed products from this reaction remain on the kaolinite surface as showed by DRIFTS, indicating that the isoprene derived products forms a layer on the mineral. This consequently can alter its ice nucleation abilities, radiative forcing, and atmospheric lifetimes in ways yet to be predicted. Overall, these findings reinforces that mineral dust affects the total trace gas budget, provides an atmospheric sink for isoprene, and the heterogeneous reaction of isoprene can extend to altering the properties of mineral dust, all of which has greater impact on the climate as a whole.

This investigation into the reactivity of isoprene with kaolinite has provided further support for the significance of studying heterogeneous reactions of isoprene. Our results yielded uptake coefficients in the $\gamma = 10^{-4}$ range under dry conditions. Previously isoprene uptake coefficients for pH 3 water surfaces estimated to be in the $\gamma = 10^{-6}$ range (Enami et al. 2012 a). Terpenes were found to have greater uptake coefficients in similar studies that were in the range of $\gamma = 10^{-3} - 10^{-5}$ on acidic surfaces and provides support for the significance of uptake on these surfaces. (Enami et al., 2012 b). Our study calculated a reactive uptake coefficient for isoprene in the 10^{-4} order of magnitude, indicating that

the reactive uptake of isoprene by mineral dust is an important process to include when considering viable isoprene sinks. Further studies performed at 15% relative humidity are underway to determine the significance of this heterogeneous reaction under atmospherically relevant conditions. Our results provide evidence for significant uptake of isoprene on mineral dust surfaces and can be extrapolated to the importance of this process in the atmosphere. This has implications on both isoprene emission levels and chemical properties of mineral dust. The uptake process consumes isoprene in the reaction process supplying support to the hypothesis that reactions with mineral dust in forest floors may be an important component in the isoprene emission discrepancy.

4.2 Atmospheric Implications

The uptake coefficient calculated under dry conditions implies that the isoprene and kaolinite reaction may be atmospherically significant. Further testing under atmospherically relevant conditions is required to assess the full significance. These conditions include adding HNO_3 (g), or NH_3 (g) which may replenish active sites on kaolinite thus increasing isoprene's reactivity especially at relative humidity which forms a water monolayer that would otherwise inhibit reactions. Expanding the project to include relative humidity would also greatly increase the atmospheric relevance of these reactions. However, preliminary studies have shown that under relative humidity, the uptake greatly diminishes due to saturation by water on the kaolinite surface. Even though the reaction of isoprene with clay minerals may not account for the missing sink, it still is a relevant process occurring in the atmosphere. Due to the abundancy of

isoprene, any reaction can significant by its production of other organic compounds and through alteration of the properties of other reactants. These results imply that heterogeneous reactions of isoprene with mineral clays produce the 2-methyl tetrol which is a known contributor to SOA. Therefore, it is possible that the 2-methyl tetrol found in atmospheric samples are a result from the reaction of isoprene and clay minerals. This reaction also has implications on mineral dust chemical properties which in turn can affect the Earth's radiation budget, cloud formation, and climate as a whole. Overall, the heterogeneous reaction of isoprene and kaolinite may be an important process in the atmosphere that requires further investigation. Future work using other components found in soil, such as illite, montmorillonite, and calcite would expand the level of understanding we have on the heterogeneous reactions of isoprene and provide a more comprehensive picture of its interactions in the atmosphere. It would also be beneficial to study the reaction between isoprene and soil to determine the overall effect the reaction between isoprene and the forest floor has on isoprene emission levels. Due to the large decrease in isoprene emission at night, studies should be expanded beyond dark conditions to include light at set wavelengths to further mimic actual atmospheric conditions.

The atmosphere is currently undergoing a massive change, and therefore so is the climate. As the source of much of this change, humans have the responsibility to stop massive changes which requires a deep understanding of all the atmospheric process that can occur and how they relate to one another. Much is already known about these processes, but a lot of unknowns still remain. It was the goal of this project to identify

one of these unknowns, which was the heterogeneous reaction of isoprene and kaolinite. Overall, we have identified the reaction between isoprene and kaolinite as a viable reaction, while also developing an exceptional experimental method for determining kinetic of heterogeneous reactions.

Bibliography

Carlton, A. G.; Wiedinmyer, C.; Kroll, J. H., A review of Secondary Organic Aerosol (SOA) formation from isoprene. *Atmos. Chem. Phys.* **2009,** *9*, 4987-5005.

Claeys, M.; Graham, B.; Vas, G.; Wang, W.; Vermeylen, R.; Pashynska, V.; Cafmeyer, J.; Guyon, P.; Andreae, M. O.; Artaxo, P.; Maenhaut, W., Formation of Secondary Organic Aerosols Through Photooxidation of Isoprene *Science* **2004,** *303*.

Cleveland, C. C.; Yavitt, J. B., Microbial Consumption of Atmospheric Isoprene in a Temperate Forest Soil *Appl. Environ. Microbiol.* **1998,** *64* (1), 172-177.

Usher, C. R.; Michel, A. E.; Grassian*, V. H., Reactions on Mineral Dust. **2003,** *103*, 4883-4940.

Crank, J., *The Mathematics of Diffusion*. Oxford University Press: London, 1975.

D'Andrea, S. D.; Häkkinen, S. A. K.; Westervelt, D. M.; C., K.; Levin, E. J. T.; Kanawade, V. P.; Leaitch, W. R.; V., S. D.; Riipinen, I.; Pierce, J. R., Understanding global secondary organic aerosol amount and size-resolved condensational behavior *Atmos. Chem. Phys* **2013,** *13*, 11519–11534.

Enami, S.; Hoffmann, M. R.; Colussi, A., Dry Deposition of Biogenic Terpenes via Cationic Oligomerization on Environmental Aqueous Surfaces *J. Phys. Chem. Lett* **2012,** (3), 3102-3108.

Enami, S.; Mishra, H.; Hoffmann, M. R.; Colussi, A. J., Protonation and Oligomerization of Gaseous Isoprene on Mildly Acidic Surfaces: Implications for Atmospheric Chemistry *J. Phys. Chem. A.* **2012,** *116*, 6027-6032.

Falkovich, A. H.; Schkolnik, G.; Ganor, E.; Rudich, Y., Adsorption of organic compounds pertinent to urban environments onto mineral dust particles. *Journal of Geophysical Research: Atmospheres (1984–2012)* **2004,** *109* (D2).

Guenther, A.; Karl, T.; Harley, P.; Wiedinmyer, C.; Palmer, P. I.; Geron, C., Estimates of global terrestrial isoprene emissions using MEGAN (Model of Emissions of Gases and Aerosols from Nature).*Atmos. Chem. Phys* **2006,** *6*, 3181-3210.

Henze, D. K.; Seinfeld, J. H., Global secondary organic aerosol from isoprene oxidation. *Geophysical Research Letters* **2006,** *33* (9).

Huysmans, M.; Dassargues, A., Review of the use of Péclet numbers to determine the relative importance of advection and diffusion in low permeability environments *Hydrogeology Journal* **2004,** *10*.

Jacob, D. J., Heterogeneous chemistry and tropospheric ozone. *Atmospheric Environment* **2000,** *34*, 2131-2159.

Kanakidou, M.; Seinfeld, J. H.; Pandis, S. N.; Barnes, I.; Dentener, F. J.; Facchini, M. C.; Dingenen, R. V.; Ervens, B.; Nenes, A. N.; Nielsen, C. J.; E., S., Organic aerosol and global climate modelling: a review. *Atmos. Chem. Phys.* **2005,** *5*, 1053–1123.

Knopf, D. A.; Poschl, U.; Shiraiwa, M., Radial Diffusion and Penetration of Gas Molecules and Aerosol Particles through Laminar Flow Reactors, Denuders, and Sampling Tubes. *Anal. Chem.* **2015,** *87*, 3746-3754.

Kolb, C. E.; Cox, R. A.; Abbatt, J. P. D.; Ammann, M.; Davis, E. J.; Donaldson, D. J.; Garrett, B. C.; George, C.; Griffiths, P. T.; Hanson, D. R.; Kulmala, M.; McFiggans, G.; Pöschl, U.; Riipinen, I.; Rossi, M. J.; Rudich, Y.; Wagner, P. E.; Winkler, P. M.; Worsnop, D. R.; Dowd, C. D. O., An overview of current issues in the uptake of atmospheric trace gases by aerosols and clouds. *Atmospheric Chemistry and Physics* **2010,** *10* (21), 10561-10605.

Kourtchev, I.; Ruuskanen, T.; Maenhaut, W.; Kulmala, M.; Claeys, M., Observation of 2-methyltetrols and related photo-oxidation products of isoprene in boreal forest aerosols from Hyytiala, Finland *Atmos. Chem. Phys.* **2005,** *5*, 2761–2770.

Kroll, J. H.; Ng, N. L.; Murphy, S. M.; Flagan, R. C.; Seinfeld, J. H., Secondary organic aerosol formation from isoprene photooxidationunder high-NOx conditions. *Geophysical Research Letters* **2005,** *32* (18).

Lanthiere, J.; Hauglustaine, D. A.; Friend, A. D.; De Noblet-Ducoudre, N.; Viovy, N.; Folberth, G. A., Impact of climate variability and land use changes on global biogenic volatile organic compound emissions. *Atmos. Chem. Phys.* **2006,** *6*, 2129-2146.

Laothawornkitkul, J.; Taylor, J. E.; Paul, N. D.; C.N., H., Biogenic Volatile Organic Compounds in the Earth System. *New Phytologist* **2009,** *183*, 27-51.

Lederer, M. A Mechanistic and Kinetic Comparison of the Reactivity of Volatile Organic Compounds on Mineral Dusts. Honors Tehsis 2016.

Liggio, J.; Li, S. M., Reactive uptake of pinonaldehyde on acidic aerosols. *J. Geophys. Res* **2006,** *111*, D24303.

Mohler, O.; Benz, S.; Saathoff, H.; Schnaiter, M.; Wagner, R.; Schneider, J.; Walter, S.; Ebert, V.; Wagner, S., The effect of organic coating on the heterogeneous ice nucleation efficiency of mineral dust aerosols. *Environ. Res. Lett.* **2008**.

Müller, J. F.; Stavrakou, T.; Wallens, S.; Smedt, I.; Roozendael, M. V.; Potosnak, M. J.; Rinne, J.; Goldstein, A.; Guenther, A. B., Global isoprene emissions estimated using MEGAN, ECMWF analyses and a detailed canopy environment model. *Atmospheric Chemistry and Physics* **2008,** *8* (5), 1329-1341.

Pöschl, U.; Martin, S. T.; Sinha, B.; Chen, Q.; Gunthe, S. S.; Huffman, J. A.; Borrmann, S.; Farmer, D. K.; Garland, R. M.; Helas, J.; Jimenez, J. L.; King, S. M.; Manzi, A.; Mikhailov, E.; Pauliquevis, T.; Petters, M. D.; Prenni, A. J.; Roldin, P.; Rose, D.; Schneider, J.; Su, H.; Zorn, S. R.; Artaxo, P.; Andreae, M. O., Rainforest Aerosols as Biogenic Nuclei of Clouds and Precipitation in the Amazon *Science* **2010,** *329*, 1513-1515.

Prather, K. A.; Hatch, C. D.; Grassian, V. H., Analysis of Atmospheric Aerosols. *Annu. Rev. Anal. Chem.* **2008,** *1*, 485-514.

Prenni, A. J.; Petters, M. D.; Faulhaber, A.; Carrico, C. M.; Ziemann, P. J.; Kreidenweis, S. M.; DeMott, P. J., Heterogeneous ice nucleation measurements of secondary organic aerosol generated from ozonolysis of alkenes *GeoPhys. Res. Lett.* **2009,** *36*.

Prospero, J. M., Long-term measurements of the transport of African mineral dust to the southeastern United States: Implications for regional air quality *J GEOPHYS RES* **1999,** *104*, 15917-15927.

Sharkey, T. D.; Wiberley, A. E.; Donohue, A. R., Isoprene Emission from Plants: Why and How. *Annals of Botany* **2008,** *101*, 5-18

Shen, X.; Zhao, Y.; Chen, Z.; Huang, D., Heterogeneous reactions of volatile organic compounds in the atmosphere. *Atmospheric Environment* **2013,** *68* (April 2013), 17.

Tang, M. J.; Shirai, M.; Poschl, R. A.; Cox, R. A.; Kalberer, M., Compilation and evaluation of gas phase diffusion coefficients of reactive trace gases in the atmosphere: Volume 2. Diffusivities of organic compounds, pressure-normalised mean free paths, and average Knudsen numbers for gas uptake calculations *Atmos. Chem. Phys.* **2015,** *15*, 5585–5598.

Todd, M.; Bou Karam, D.; Cavazos, C.; Bouet, C.; Heinold, B.; Baldasano, J.; Cautenet, G.; Koren, I.; Perez, C.; Solmon, F.; Tegen, I., Quantifying uncertainty in estimates of mineral dust flux: An intercomparison of model performance over the Bodélé Depression, northern Chad. . *J. Geophys. Res.* **2008,** *113*.

Ulery, A.; Drees, R., *Methods of Soil Analysis: Mineralogical methods*. American Society of Agronomy: 2008; Vol. 5.

Usher, C. R.; Michel, A. E.; Grassian, V. H., Reactions on Mineral Dust. *Chem. Rev.* **2003,** *103*, 4883-4939.

Wang, B.; Lambe, A. T.; Massoli, P.; Onasch, T. B.; Davidovits, P.; Worsnop, D. R.; Knopf, D. A., The deposition ice nucleation and immersion freezing potential of amorphous secondary organic aerosol: Pathways for ice and mixed-phase cloud formation *J. Geophys. Res.* **2012,** *117*.

Ying, Q.; Li, J.; Kota, S. H., Significant Contributions of Isoprene to Summertime Secondary Organic Aerosol in Eastern United States. *Environ. Sci. Technol.* **2015,** *49*, 7834-7842.

Zhang, J.; Sundar, C. A., Longwave radiative forcing of Saharan dust aerosols estimated from MODIS, MISR, and CERES observations on Terra *Geophys. Res. Lett.* **2003,** *30*.